DISSERTATION

VIBRATION OF NANOSTRUCTURES: FROM ATOMIC TO CONTINUUM SCALES

Submitted by
Fernando Ramirez
Department of Civil Engineering

In partial fulfillment of the requirements
For the Degree of Doctor of Philosophy
Colorado State University
Fort Collins, Colorado
Summer 2006

COLORADO STATE UNIVERSITY

April 11, 2006

WE HEREBY RECOMMEND THAT THE DISSERTATION VIBRATION OF NANOSTRUCTURES: FROM ATOMIC TO CONTINUUM SCALES PREPARED UNDER OUR SUPERVISION BY FERNANDO RAMIREZ R. BE ACCEPTED AS FULFILLING IN PARTIAL REQUIREMENTS FOR THE DEGREE OF DOCTOR OF PHILOSOPHY.

Committee on Graduate Work

Marvin E. Criswell, Committee Member

Robert G. Leisure, Committee Member

Anthony K. Rappe, Committee Member

Paul R. Heyliger, Adviser

Luis Garcia, Department Head

ABSTRACT OF DISSERTATION

VIBRATION OF NANOSTRUCTURES: FROM ATOMIC TO CONTINUUM SCALES

One of the most important and challenging characteristics of nanostructures is the size-dependence that the properties of these materials and components exhibit from what is known as the quantum size effect. The most suitable models to study the behavior of particles at this very small scale are the computationally expensive methods of quantum mechanics and molecular dynamics. At the other end of the scale spectrum, continuum mechanics methods are computationally much faster, but they do not explicitly consider atomic and electronic interactions that may affect the properties of these novel structures which, below a certain scale, cannot be considered as continuum solids.

In this study, vibrational frequency spectra of sphere-, cube-, tetrahedron-, and pyramid-shape nanoparticles made of silicon, germanium, and carbon were computed using three different models. The three methods span the range of length scales starting from molecular mechanics at the atomic level, passing through a modified molecular dynamics approach, and continuing on to the continuum level in which the nanoparticles are considered as solid elastic structures.

The dependence of the natural frequencies of particles on the size at the nanoscale was confirmed, the magnitude of the frequencies and the number and location of

degenerate frequencies change with particle size. Normalized frequencies increase non-linearly as the number of atoms forming the particle is increased, while they increase linearly as a function of the particle size. The latter indicates that the scale invariance of the normalized frequencies in continuum elasticity does not hold for the range of particles sizes considered in this study.

First and second order polynomials were proposed to describe the variation of the lowest normalized frequency as a function of the size, and of the number atoms forming the particles, respectively. The converged frequency values using the second order polynomials only differ about -2% for silicon particles compared to continuum mechanics results for cubic material symmetry, while the differences are about +20% and -15% for germanium and carbon nanostructures. Therefore, the applicability of the continuum mechanics assumption at this scale depends not only on the size, but also on the material of which the nanostructures are composed.

Fernando Ramirez
Department of Civil Engineering
Colorado State University
Fort Collins, Colorado 80523-1372
Summer 2006

Contents

List of Figures

List of Tables

Chapter 1
Introduction

The advance of science and technology has reached the nanotechnology era. In the past decade, significant advances have been achieved in the area of nanoengineering. The existence of numerous different types of nanostructures have been reported in the literature, including nanoparticles or quantum dots, single- and multi-walled nanotubes, nanowires, and nanoropes. One of the most important characteristics of nanostructures is the size-dependence that the properties of these materials and components exhibit. Due to the extremely small size of these structures, the development of efficient methods to evaluate their electronic, mechanical, optical, and acoustical properties is a challenge to researchers.

Different methods have been employed for the determination of the properties of nanostructures. They can be divided into two main categories: atomistic models and elastic continuum model theories. Atomistic approaches include both classical quantum mechanics and molecular dynamics and mechanics. In principle, these are the most suitable methods to deal with molecular or atomic motions. However, the application of atomistic models are computationally expensive, and their application is limited to nanostructures formed by a small number of molecules or atoms. On the other hand, continuum mechanics approaches are computationally much faster, but they do not explicitly consider atomic and electronic interactions that may affect the properties of these novel structures. At these very small length scales, these nanostructures cannot be considered continuous and the validity of classical continuum

approaches must be evaluated and potentially modified.

In this study, the vibrational frequency spectra of nanoparticles with different shapes are to be evaluated using three different models. The geometries to be considered correspond to cube-, sphere-, tetrahedron- and pyramid-shaped nanostructures. The three methods to be employed span a range of length scales starting from molecular mechanics at the atomic level, passing through a modified molecular dynamics approach, and going to the continuum level in which the nanoparticles are considered as solid elastic structures.

The main objectives of this work are to 1) determine the validity of the modified molecular dynamics and continuum approaches for the evaluation of vibration frequencies of the solids as their size tends towards the nanoscale, and 2) obtain equations that allow the prediction of the natural frequencies of nanostructures as a function of the number of atoms forming the particles, and as a function of the particle size.

This dissertation is organized as follows: first, a brief literature review is presented. Then, each of the proposed computational models is shortly explained, followed by the analysis and presentation of the obtained results. Finally, the summary and conclusions derived from this work are outlined.

Chapter 2
Literature Review

Nanoparticles or quantum dot heterostructures are used widely in a number of advanced semiconductor devices including quantum dot semiconductor lasers. Additionally, recent investigations predict extensive applications in biology, bioengineering, and medicine as biological tags and as active electrical contacts to neurons [1]. Nanoparticles show optical and acoustic properties different from those of the bulk crystals of the same material. These differences are attributed to the three-dimensional confinement of electrons and holes in small volumes known as quantum size effect [2]. There exist several studies in which the acoustic modes of nanoparticles have been evaluated. Tamura et al. [3] used an extension of Lamb's theory [4] of the vibration of homogeneous and free standing elastic spheres to study the matrix, surface relaxation, and local clamping effects on the eigenfrequencies of small particles. Tanaka et al. [5] reported results from experiment on low-frequency Raman scattering from CdS microcrystals of various sizes embedded in a germanium dioxide glass matrix. They found that the Lamb's theory assumption of considering the nanoparticle as a homogeneous elastic body is reasonable if the CdS microcrystal is large enough (diameter larger than 7.5 nm). Ovisuk and Novikov [6] also used low-frequency Raman scattering to show the significant influence that a glass matrix have on the spheroidal and torsional modes of microcrystals. Verma et al. [7] presented a theoretical model based on classical elasticity theory to establish the relationship between particle size, the frequency, and the width of various confined phonons, obtaining good

agreement with experimental results for the case of $CdS_xSe_1 - x$ nanoparticles embedded in a glass matrix. Saviot et al. [8] reported the size-dependence of acoustic and optical vibrational modes of CdSe nanocrystals in a glass matrix using low-frequency Raman scattering. More recently, Saviot et al. [9] studied the vibrations of free and embedded anisotropic elastic spheres, more specifically, silicon nanoparticles in a silica matrix. They used low-frequency Raman scattering, an analytical solution based on continuum elasticity, and a molecular dynamics approach. They reported that the silica matrix has three effects: it shifts energies, it creates damping, and it also introduces new vibrational modes.

Most of the previously mentioned studies reported good agreement between experimental measurements of the natural frequencies of spherical nanoparticles and those obtained using theoretical models based on continuum elasticity. However, this agreement was only valid for particles with diameter larger than 7.5 nm [5], or for particles having a large enough diameter to satisfy the scale invariance of the frequency-radius product holding for continuum elasticity. In the present study the natural vibration frequencies of free standing silicon, germanium, and carbon nanoparticles are calculated using three different methods: molecular mechanics (at the atomic level), molecular dynamics (at a "quasi-continuum" level), and classical elasticity (at the continuum level). Four different geometries are studied: cubes, spheres, tetrahedrons, and pyramids. Isotropic and cubic material behaviors are both considered. Once the frequency spectra have been obtained, the particle size range for which the assumptions of continuum elasticity are valid is intended to be determined. Equations describing the variation of the natural frequencies as a function of the number

of atoms forming the nanoparticles are also constructed. The specific contributions of this work are presented below, along with the current scientific advance.

1. Evaluation of the free vibration of free standing sphere-, cube-, and tetrahedron-shaped silicon, germanium, and carbon nanoparticles. To the knowledge of the author, only vibrational spectra for spherical nanostructures have been reported in the literature.

2. Evaluation of the applicability of continuum elastic, and modified molecular dynamics models for the determination of the natural frequencies of free standing particles with different size, shapes, and made of different materials as their size tends towards the nanoscale. Only one work has been reported in this area, and only for spherical particles [5].

3. Determination of analytical expressions to evaluate the natural frequencies of silicon, germanium, and carbon nanoparticles with different shapes as functions of the number of atoms forming the molecules, and as functions of the size of the nanoparticle. These expressions can be used to estimate changes in elastic constants as the particle size decreases. To the best knowledge of the author, these type of equations have not been reported before

Chapter 3
Theoretical and Computational tools

3.1 The Atomic Model

Molecular mechanics is a simple, empirically-based "ball-spring" atomistic model for molecular structures. Atoms are connected by bonds that can be stretched or compressed due to intra- or inter-molecular forces. The size of the atoms and the stiffness of the bonds are determined empirically by being chosen to reproduce experimental data. The force field/molecular mechanics model evaluates the potential energy, V, for a molecule as the sum of energies from two, three, and four-body interactions [20], and can be expressed as

$$V = V_r + V_\theta + V_\phi + V_\omega + V_{vdW} + V_{el} \tag{3.1}$$

The first four energies on the right-hand side of this equation are related to bond stretching, bond angle bending, dihedral angle torsion, and inversion terms, respectively. The nonbonded energies include van der Waals and electrostatic contributions, and they are represented by the final two terms on the right-hand side. The total potential energy gives a mathematical representation for how each atom would move under the influence of the motions of all the other atoms in the system. Vibrational frequencies are determined using molecular mechanics by determining the equilibrium geometry from energy minimization, and then using a harmonic oscillator approximation to reproduce the vibrational frequencies. Expressions for the different terms that contribute to the total potential energy are functions of the atomic positions, inter-atomic equilibrium distances, and different parameters that are obtained and

calibrated by fitting experimental data and quantum mechanics results.

In this study, the Approximate Pair Theory (APT) developed in the Department of Chemistry at Colorado State University is used to calculate the vibrational spectra of particles at the nanoscale. APT uses parametric models of electronic interactions to permit reasonable descriptions of the electronic changes associated with nanoscale chemistry. This theory makes use of the force field developed by Rappe et. al [10] and known as the universal force field (UFF). The UFF is a set simple functional forms and parameters used to model the structure, movement, and interactions of molecules. The parameters are defined empirically or by combining atomic parameters according to certain rules. A more detailed description of this process may be found elsewhere [10-13].

In this study the focus is on silicon, germanium, and carbon particles for which the different energy terms are presented below.

For the bond stretch term, an Extended Rydberg function (Murrell and Sorbie 1974 [14]; Huxley and Murrell 1983 [15]) is used as shown by

$$V_r = -D_e BO\,(IJ) \tag{3.2}$$

where D_e is 85.0, 70.0, and 99.0 kcal/mol for silicon, germanium, and carbon respectively, and the bond order BO is given by

$$BO\,(IJ) = e^{-4\alpha_{ij}(r-r_{IJ})}\left[1 + 4\alpha_{IJ}\,(r - r_{IJ})\left[1 + \alpha_{IJ}\,(r - r_{IJ})\left[1 + \alpha_{IJ}\,(r - r_{IJ})\right]\right]\right] \tag{3.3}$$

Here, the constants for silicon, germanium and carbon are: the bond distance pa-

rameters r_{ij} are 2.330, 2.384, and 1.480 $\mathring{A}$, respectively, and the exponents, α_{ij} are 0.6955, 0.8251, and 0.9724 $1/\mathring{A}$.

A bond-order-dependent cosine expansion is used for the angle. Bond order mediation of angular deformation terms has previously been used for the water potential surface (Ermakov, Butayev, and Spiridonov, 1990 [16]) and in the general Stillinger-Weber potential (Stillinger and Weber, 1985 [17]). It is given by

$$V_\theta = \frac{1}{2} K_\theta BO(IJ) BO(JK) \left(\cos\theta_{IJK} - \cos\theta_{0IJK}\right) \tag{3.4}$$

where the force constants K_θ for silicon, germanium, and carbon are 43.382, 58.361, and 114.657 kcal/mol, respectively, and the equilibrium angle θ_{0IJK} is 109.471^o for all elements considered.

A bond-order-dependent three-fold torsional potential is used and is given by

$$V_\phi = K_{IJKL} BO\left(IJ\right) BO\left(JK\right) BO\left(KL\right) \left(1 - \cos 3\phi_{IJKL}\right) \tag{3.5}$$

The silicon torsion parameter, K_{IJKL}, is 1.225 kcal/mol. It is 0.701 and 2.730 kcal/mol for germanium and carbon.

A Morse-Spline van der Waals potential is used for non-bonded interactions (Pack et al. 1982 [18, 19]). A Morse potential describes the inner wall region as well as the bottom of the well.

$$V_{vdW} = D_{IJ} \left(e^{-2\alpha_{IJ}(x - x_{IJ})} - 2e^{-\alpha_{IJ}(x - x_{IJ})}\right) \tag{3.6}$$

Here, dissociation energies are 0.303, 0.611, and 0.095 kcal/mol, the equilibrium distances are 4.41, 4.54, and 3.75 $\mathring{A}$, and the exponents α_{ij} are 1.266, 1.291, and 1.40 $1/\mathring{A}$, for silicon, germanium, and carbon, respectively.

Long range interactions are described by an inverse-6 potential as expressed by

$$V_{vdW} = \frac{C_6}{x^6} \tag{3.7}$$

The C6 coefficients (3689.64, 7641.02, and 473.32 $\mathring{A}^6$ kcal/mol) are selected to match the Morse potential for non-bonded interactions (Eq. 3.6) at a crossover point or cutoff distance, which is selected to provide continuous first derivatives.

The molecular mechanics calculations begin with the determination of the minimized or equilibrium molecular structures, which correspond to the lowest possible energy level. The equilibrium coordinates for each atom within the molecule are obtained by energy minimization using the Newton-Raphson minimization technique [20]. In the Newton-Raphson algorithm, both the gradient of the potential energy $\nabla \mathbf{V}$ (where we use bold-face to denote a vector), and the second derivative or Hessian matrix, $\mathbf{H_V}$, are evaluated at the initial trial geometry $\mathbf{r_o}$. Since the Hessian matrix defines the curvature of the potential energy surface in each gradient direction, multiplication of this matrix by the gradient results in a vector which translates the system towards the minimum at $\mathbf{r_{min}}$. The general expression describing this procedure is expressed as

$$\mathbf{r_{min}} = \mathbf{r_o} - \mathbf{H_V^{-1}} \nabla \mathbf{V} \tag{3.8}$$

The evaluation of the natural vibration frequencies begins with the expression for the total kinetic energy (T) of the n-atom system given by (see Wilson et al. [21])

$$T = \frac{1}{2}\sum_{\alpha=1}^{n}\sum_{i=1}^{3} m_\alpha \left(\frac{d\Delta x_i^\alpha}{dt}\right)^2 = \frac{1}{2}\sum_{\alpha=1}^{n}\sum_{i=1}^{3} m_\alpha \left(\frac{q_i^\alpha}{dt}\right)^2 = \frac{1}{2}\sum_{\alpha=1}^{n}\sum_{i=1}^{3} \dot{q}_i^\alpha \tag{3.9}$$

where m_α is the mass of atom α, Δx_i^α is its displacement in the j^{th} coordinate direction relative to the equilibrium position, q_i^α is its mass-weighted displacement $\sqrt{m_\alpha}\Delta x_i^\alpha$, and t is time. For small vibrations, the potential energy may be expressed as a power series in the displacement q_i^α

$$V = V_o + \sum_{\alpha=1}^{n}\sum_{i=1}^{3}\left(\frac{\partial V}{\partial q_i^\alpha}\right)_o q_i^\alpha + \sum_{\alpha,\beta=1}^{n}\sum_{i,j=1}^{3}\left(\frac{\partial^2 V}{\partial q_i^\alpha \partial q_j^\beta}\right)_o q_i^\alpha q_j^\beta + O(x_i)^3 \tag{3.10}$$

By selecting the zero energy at the equilibrium configuration, and considering that the corresponding gradient of the potential energy is a minimum, V_o and $(\partial V/\partial q_i^\alpha)_o$ may be respectively eliminated, neglecting the higher order terms under the small displacements assumption, Equation 3.10 becomes

$$V = \sum_{\alpha,\beta=1}^{n}\sum_{i,j=1}^{3}\left(\frac{\partial^2 V}{\partial q_i^\alpha \partial q_j^\beta}\right)_o q_i^\alpha q_j^\beta \tag{3.11}$$

The Euler-Lagrange equation is given by

$$\frac{d}{dt}\frac{\partial T}{\partial \dot{q}_j^\alpha} + \frac{\partial V}{\partial q_j^\alpha} = 0 \tag{3.12}$$

Since T is a function of the velocities only, and V is a function of the coordinates only, substitution of them in Equation 3.12 yields the equations

$$\ddot{q}_j^\alpha + \sum_{\alpha,\beta=1}^{n} \sum_{i,j=1}^{3} \left(\frac{\partial^2 V}{\partial q_i^\alpha \partial q_j^\beta} \right)_o q_i^\alpha = 0 \tag{3.13}$$

This is a system of 3n simultaneous second-order linear differential equations. The terms $(\partial^2 V / \partial x_i^\alpha \partial x_j^\beta)$ are constants evaluated at the equilibrium configuration. Assuming harmonic motion, Equation 3.13 takes the form of an eigenvalue problem that can be solved using conventional methods, i.e.

$$[F]\{x\} = \omega^2 [M]\{x\} \tag{3.14}$$

where ω and the vector $\mathbf{x}$ represent the frequencies and corresponding eigenvectors respectively, and the elements of the stiffness matrix [F], and the diagonal mass matrix [M] are given by

$$F_{ij}^{\alpha\beta} = \left(\frac{\partial^2 V}{\partial q_i^\alpha \partial q_j^\beta} \right)_o \tag{3.15}$$

$$M_{ii}^{\alpha} = m_\alpha \tag{3.16}$$

The General Molecular Incorporated molecular modeling software package available through the Department of Chemistry at Colorado State University was employed to evaluate the natural frequencies and corresponding mode shapes of the nanoparticles using the molecular mechanics method. This software consists of a set of interactive and batch modules with which molecular structures can be created,

displayed, edited, and minimized, and the vibrational characteristics (normal modes and vibrational frequencies) of a molecular system can also be generated.

3.2 The Molecular Dynamics Model

The molecular model used in this study is based on the molecular dynamics calculation presented by Saviot et al. [22]. In their approach, a solid of arbitrary shape is modeled by constructing a crystal cubic lattice from mass points connected by springs. Each particle with mass ρa^3 and position $\mathbf{r}_j$, where a is the lattice constant, has six first neighbors, twelve second neighbors, eight third neighbors, and so on. The potential energy U coupling every pair (i, j) of first, second, third, fourth, fifth neighbors is expressed by the following relations

$$U_{1^{st}} = (1/2)k_{sp1}\left(\|\mathbf{r}_i - \mathbf{r}_j\| - a\right)^2 \tag{3.17}$$

$$U_{2^{nd}} = (1/2)k_{sp2}\left(\|\mathbf{r}_i - \mathbf{r}_j\| - \sqrt{2}a\right)^2 \tag{3.18}$$

$$U_{3^{rd}} = (1/2)k_{sp3}\left(\|\mathbf{r}_i - \mathbf{r}_j\| - \sqrt{3}a\right)^2 \tag{3.19}$$

$$U_{4^{th}} = (1/2)k_{sp4}\left(\|\mathbf{r}_i - \mathbf{r}_j\| - \sqrt{4}a\right)^2 \tag{3.20}$$

$$U_{5^{th}} = (1/2)k_{sp5}\left(\|\mathbf{r}_i - \mathbf{r}_j\| - \sqrt{5}a\right)^2 \tag{3.21}$$

There is also an eight point force term involving a constant k_{8pt}. This force is not calculated for pairs, but for cubic groups of eight atoms. The energy relating cubic octets is given by

$$U_{8pt} = \left(k_{8pt}/4a^2\right)\left(D - 6a^2\right)^2$$

$$D = \sum_{j=1}^{8} \|\mathbf{R}_{cm} - \mathbf{r}_j\|^2 \tag{3.22}$$

$$\mathbf{R}_{cm} = (1/8) \sum_{j=1}^{8} \mathbf{r}_j$$

The next step in their model is to relate the force constants in Equations 3.17-3.22 to the bulk elastic constants of the material. Saviot et al. showed that only three interaction terms are required to exactly fit the three elastic parameters C_{11}, C_{12}, and C_{44} of a general cubically elastic material. The terms for a cubic material with a Zener anisotropy ratio ($A = 2C_{44}/(C_{11} - C_{12})$ below 2 correspond to the first, second, and octet neighbor interactions. The force constants are determined from the energy stored in a solid due to a small dilatation, and from the speed of transverse and longitudinal plane waves moving along the x-axis of the solid. They are given by

$$k_{sp1} = a(C_{11} - (C_{12} + C_{44}) \tag{3.23}$$

$$k_{sp2} = aC_{44} \tag{3.24}$$

$$k_{8pt} = (1/8)a(C_{12} - C_{44}) \tag{3.25}$$

For the case of materials with Zener anisotropy above 2, the three terms correspond to first, third, and octet neighbor interactions. Expressions for the force constants, as well as a detailed explanation of their derivation can be found elsewhere [22].

Our approach begins with the functions describing the potential energy interactions given by Equations 3.17, 3.18, and 3.22. We then express the position vectors of the mass points at any time in terms of their initial coordinates (x, y, z) and their corresponding displacements (u, v, w) as

$$\mathbf{r} = (x+u)\hat{i} + (y+v)\hat{j} + (z+w)\hat{k} \tag{3.26}$$

The absolute distance between two pair of particles is then given by

$$\|\mathbf{r}_i - \mathbf{r}_j\| = \Big[(x_i - x_j + u_i - u_j)^2 + (y_i - y_j + v_i - v_j)^2 + (z_i - z_j + w_i - w_j)^2\Big]^{1/2} \tag{3.27}$$

Substituting Equation 3.27 back into Equations 3.17 and 3.18, neglecting higher order terms on u, v, and w based on the assumption of small displacements, and using the binomial expansion, the potential energy equations corresponding to first and second neighbor interactions result in

$$U_{1^{st}} = \frac{K_{sp1}}{2a^2}\left[(x_i - x_j)(u_i - u_j) + (y_i - y_j)(v_i - v_j) + (z_i - z_j)(w_i - w_j)\right]^2 \tag{3.28}$$

$$U_{2^{nd}} = \frac{K_{sp2}}{4a^2}\left[(x_i - x_j)(u_i - u_j) + (y_i - y_j)(v_i - v_j) + (z_i - z_j)(w_i - w_j)\right]^2 \tag{3.29}$$

For the case of octet interaction we use Equation 3.27 to express the D and $6a^2$ terms in the octet potential energy as

$$D = \sum_{i=1}^{8}\left[0.125\sum_{j=1}^{8}(x_j + u_j) - (x_i - u_i)\right]^2 + \sum_{i=1}^{8}\left[0.125\sum_{j=1}^{8}(y_j + v_j) - (y_i - v_i)\right]^2 + \sum_{i=1}^{8}\left[0.125\sum_{j=1}^{8}(z_j + w_j) - (z_i - w_i)\right]^2 \tag{3.30}$$

$$6a^2 = \sum_{i=1}^{8}\left(0.125\sum_{j=1}^{8}x_j - x_i\right)^2 + \sum_{i=1}^{8}\left(0.125\sum_{j=1}^{8}y_j - y_i\right)^2 + \tag{3.31}$$

$$\sum_{i=1}^{8}\left(0.125\sum_{j=1}^{8}z_j - z_i\right)^2$$

Substituting Equations 3.30 and 3.31 back into Equation 3.22, the potential energy corresponding to octet interactions becomes

$$U_{8pt} = \left(k_{8pt}/4a^2\right)\left[\left\{D = \sum_{i=1}^{8}\left[0.125\sum_{j=1}^{8}(x_j+u_j) - (x_i-u_i)\right]^2 + \sum_{i=1}^{8}\left[0.125\sum_{j=1}^{8}(y_j+v_j) - (y_i-v_i)\right]^2 + \sum_{i=1}^{8}\left[0.125\sum_{j=1}^{8}(z_j+w_j) - (z_i-w_i)\right]^2\right\} - \left\{\sum_{i=1}^{8}\left(0.125\sum_{j=1}^{8}x_j - x_i\right)^2 + \sum_{i=1}^{8}\left(0.125\sum_{j=1}^{8}y_j - y_i\right)^2 + \sum_{i=1}^{8}\left(0.125\sum_{j=1}^{8}z_j - z_i\right)^2\right\}\right]^2 \tag{3.32}$$

The kinetic energy (T) of the system comprising all the mass points (m) in the solid is given by

$$T = \frac{1}{2}\sum_{\alpha=1}^{m}\sum_{i=1}^{3}m_\alpha\left(\frac{du_i^\alpha}{dt}\right)^2 \tag{3.33}$$

where u_i^α is the displacement of mass point α in the i^{th} coordinate direction, and m_α is the mass of the particle.

In order to obtain the final equations for the calculation of the natural frequencies of the nanoparticles, we make use of the Euler-Lagrange equation again which is rewritten here for the current notation as

$$\frac{d}{dt}\frac{\partial T}{\partial \dot{u}_i} + \frac{\partial U}{\partial u_i} = 0 \tag{3.34}$$

The free vibration of the solids is developed assuming harmonic motion. Solutions for the primary unknowns have the form

$$u(x,y,z,t) = u(x,y,z)e^{i\omega t} \tag{3.35}$$

$$v(x,y,z,t) = v(x,y,z)e^{i\omega t} \tag{3.36}$$

$$w(x,y,z,t) = w(x,y,z)e^{i\omega t} \tag{3.37}$$

where ω is the natural frequency. Taking second derivative with respect to time of Equations 3.35 to 3.37 gives

$$\ddot{u}_i(x,y,z,t) = -\omega^2 u_i(x,y,z)e^{i\omega t} \tag{3.38}$$

$$\ddot{v}_i(x,y,z,t) = -\omega^2 v_i(x,y,z)e^{i\omega t} \tag{3.39}$$

$$\ddot{w}_i(x,y,z,t) = -\omega^2 w_i(x,y,z)e^{i\omega t} \tag{3.40}$$

Replacing Equations 3.28, 3.29, 3.32, and 3.35 to 3.40 into Equation 3.34 and simplifying, the dynamic problem becomes the following eigenvalue problem which is solved assuming free vibrations (i.e. no external forces) to determine the natural frequencies and the corresponding mode shapes for the different solids of interest.

$$\begin{bmatrix} [K^{uu}] & [K^{uv}] & [K^{uw}] \\ [K^{vu}] & [K^{vv}] & [K^{vw}] \\ [K^{wu}] & [K^{wv}] & [K^{ww}] \end{bmatrix} \begin{Bmatrix} \{u\} \\ \{v\} \\ \{w\} \end{Bmatrix} \tag{3.41}$$

$$-\omega^2 \begin{bmatrix} [M^{uu}] & [0] & [0] \\ [0] & [M^{vv}] & [0] \\ [0] & [0] & [M^{ww}] \end{bmatrix} \begin{Bmatrix} \{u\} \\ \{v\} \\ \{w\} \end{Bmatrix} = \begin{Bmatrix} \{0\} \\ \{0\} \\ \{0\} \end{Bmatrix}$$

here, the submatrices $[M]$ are diagonal matrices with elements ρa^3, and the submatrices $[K]$ are constructed based on Equations 3.28, 3.29, and 3.32. The contributions from first neighbor interactions can be written in matrix form as

$$\frac{k_{sp1}}{a^2}\begin{bmatrix} A^2 & -A^2 & AB & -AB & AC & -AC \\ -A^2 & A^2 & -AB & AB & -AC & AC \\ AB & -AB & B^2 & -B^2 & BC & -BC \\ -AB & AB & -B^2 & B^2 & BC & -BC \\ AC & -AC & BC & -BC & C^2 & -C^2 \\ -AC & AC & -BC & BC & -C^2 & C^2 \end{bmatrix}\begin{Bmatrix} u_i \\ u_j \\ v_i \\ v_j \\ w_i \\ w_j \end{Bmatrix} \tag{3.42}$$

Contributions from second neighbors are given by

$$\frac{k_{sp2}}{2a^2}\begin{bmatrix} A^2 & -A^2 & AB & -AB & AC & -AC \\ -A^2 & A^2 & -AB & AB & -AC & AC \\ AB & -AB & B^2 & -B^2 & BC & -BC \\ -AB & AB & -B^2 & B^2 & BC & -BC \\ AC & -AC & BC & -BC & C^2 & -C^2 \\ -AC & AC & -BC & BC & -C^2 & C^2 \end{bmatrix}\begin{Bmatrix} u_i \\ u_j \\ v_i \\ v_j \\ w_i \\ w_j \end{Bmatrix} \tag{3.43}$$

where (i, j) pairs are first neighbors in Equation 3.42 and second neighbors in Equation 3.43, and A, B, and C are given by

$$A = (x_i - x_j) \tag{3.44}$$

$$B = (y_i - y_j) \tag{3.45}$$

$$C = (z_i - z_j) \tag{3.46}$$

The contributions from octet interactions form a (8x8) square matrix for each cubic group of eight atoms. The elements of this matrix are given by

$$K_{ij} = \frac{k_{8pt}}{32a^2}(8x_j - \sum_{m=1}^{8} x_m)(8x_i - \sum_{m=1}^{8} x_m) \qquad i = 1...8, j = 1...8 \tag{3.47}$$

$$K_{ij} = \frac{k_{8pt}}{32a^2}(8y_{j-8} - \sum_{m=1}^{8} y_m)(8x_i - \sum_{m=1}^{8} x_m) \qquad i = 1...8, j = 9...16 \tag{3.48}$$

$$K_{ij} = \frac{k_{8pt}}{32a^2}(8z_{j-16} - \sum_{m=1}^{8} z_m)(8x_i - \sum_{m=1}^{8} x_m) \qquad i = 1...8, j = 17...24 \tag{3.49}$$

$$K_{ij} = \frac{k_{8pt}}{32a^2}(8x_j - \sum_{m=1}^{8} x_m)(8y_{i-8} - \sum_{m=1}^{8} y_m) \qquad i = 9...16, j = 1...8 \tag{3.50}$$

$$K_{ij} = \frac{k_{8pt}}{32a^2}(8y_{j-8} - \sum_{m=1}^{8} y_m)(8y_{i-8} - \sum_{m=1}^{8} y_m) \qquad i = 9...16, j = 9...16 \tag{3.51}$$

$$K_{ij} = \frac{k_{8pt}}{32a^2}(8z_{j-16} - \sum_{m=1}^{8} z_m)(8y_{i-8} - \sum_{m=1}^{8} y_m) \qquad i = 9...16, j = 17...24 \tag{3.52}$$

$$K_{ij} = \frac{k_{8pt}}{32a^2}(8x_j - \sum_{m=1}^{8} x_m)(8z_{i-8} - \sum_{m=1}^{8} z_m) \qquad i = 17...24, j = 1...8 \tag{3.53}$$

$$K_{ij} = \frac{k_{8pt}}{32a^2}(8y_{j-8} - \sum_{m=1}^{8} y_m)(8z_{i-8} - \sum_{m=1}^{8} z_m) \qquad i = 17...24, j = 9...16 \tag{3.54}$$

$$K_{ij} = \frac{k_{8pt}}{32a^2}(8z_{j-16} - \sum_{m=1}^{8} z_m)(8z_{i-8} - \sum_{m=1}^{8} z_m) \qquad i = 17...24, j = 17...24 \tag{3.55}$$

The molecular dynamics method presented in this section is employed to calculate the natural frequencies and vibrational modes of the nanoparticles considered in this study. For this purpose, a Fortran program was developed in which the mass and stiffness matrices for each system are first evaluated according to Equations 3.42-3.55, then, conventional eigenvalue solvers are used to calculate the frequencies and corresponding mode shapes.

3.3 The Continuum Model

The continuum approach begins with the equations of motion for a general anisotropic linearly elastic solid given by

$$\sigma_{ij,j} + f_i = \rho \frac{\partial^2 u_i}{\partial t^2} \tag{3.56}$$

Here σ_{ij}, f_i, ρ, u_i, and t denote the components of the stress tensor, the vector components of the body force, the mass density, the components of the displacements, and time respectively. Following the standard formulation used in variational solid mechanics methods, the equations of motion are multiplied by arbitrary functions that represent the virtual displacements δu_i, integrating over the volume V of the solid results in

$$\int_V \delta u_i (\sigma_{ij,j} + f_i - \rho \frac{\partial^2 u_i}{\partial t^2}) dV = 0 \tag{3.57}$$

Integrating by parts and applying the divergence theorem yields the weak form of the governing equations as

$$\int_V (\sigma_{ij} \delta \epsilon_{ij} - \delta u_i f_i + \delta u_i \rho \frac{\partial^2 u_i}{\partial t^2}) dV - \oint_S t_i \delta u_i dS = 0 \tag{3.58}$$

where t_i are the vector components of the surface tractions, and ϵ_{ij} are the components of the strain tensor which are related to the displacements and stresses by the equations

$$\epsilon_{ij} = \frac{1}{2}(u_{i,j} + u_{j,i}) \tag{3.59}$$

$$\sigma_{ij} = C_{ijkl}\epsilon_{ij} \tag{3.60}$$

Here C_{ijkl} are the components of the elastic stiffness tensor. Using the assumption of periodic motion with natural frequency denoted by ω, the components of the displacements and acceleration vectors are expressed as

$$u_i = u_i(x, y, z, t) = u_i(x, y, z)e^{i\omega t} \tag{3.61}$$

$$\frac{\partial^2 u_i}{\partial t^2} = \ddot{u}_i(x, y, z, t) = -\omega^2 u_i(x, y, z)e^{i\omega t} \tag{3.62}$$

For the problem of free vibration, there are no applied external loads, and each face of the solid is assumed to be stress free. Hence in the weak form of the governing equations there are no surface terms involving specified displacements or tractions.

Substitution of the strain-displacement relations, constitutive equations, and using the assumption of periodic motion, Equations 3.56-3.59, into the weak form (Eq. 3.55), and assuming the absence of body force yields the variational form of the governing equations for a material with at least cubic symmetry as

$$\begin{aligned}\int_V \Bigg\{ &\left[C_{11}\frac{\partial u}{\partial x} + C_{12}\frac{\partial v}{\partial y} + C_{13}\frac{\partial w}{\partial z}\right]\frac{\partial \delta u}{\partial x} + \left[C_{12}\frac{\partial u}{\partial x} + C_{22}\frac{\partial v}{\partial y} + C_{23}\frac{\partial w}{\partial z}\right]\frac{\partial \delta v}{\partial y} + \\ &\left[C_{13}\frac{\partial u}{\partial x} + C_{23}\frac{\partial v}{\partial y} + C_{33}\frac{\partial w}{\partial z}\right]\frac{\partial \delta w}{\partial z} + C_{44}\left(\frac{\partial v}{\partial z} + \frac{\partial w}{\partial y}\right)\left(\frac{\partial \delta v}{\partial z} + \frac{\partial \delta w}{\partial y}\right) + \\ &C_{55}\left(\frac{\partial u}{\partial z} + \frac{\partial w}{\partial x}\right)\left(\frac{\partial \delta u}{\partial z} + \frac{\partial \delta w}{\partial x}\right) + C_{66}\left(\frac{\partial u}{\partial y} + \frac{\partial v}{\partial x}\right)\left(\frac{\partial \delta u}{\partial y} + \frac{\partial \delta v}{\partial x}\right)\Bigg\} dV - \\ &\int_V \omega^2 \rho \left(u\delta u + v\delta v + z\delta w\right) dV = 0\end{aligned} \tag{3.63}$$

Rather than directly solving the governing differential equations, the Ritz method (see [23]) seeks approximate solutions to the weak forms of these equations. This is accomplished by approximating the displacement components and their variations using finite linear combinations of the form

$$u(x,y,z) = \phi_0^u(x,y,z) + \sum_{j=1}^{n} a_j \phi_j^u(x,y,z) \tag{3.64}$$

$$v(x,y,z) = \phi_0^v(x.y.z) + \sum_{j=1}^{n} b_j \phi_j^v(x,y,z) \tag{3.65}$$

$$w(x,y,z) = \phi_0^w(x,y,z) + \sum_{j=1}^{n} d_j \phi_j^w(x,y,z) \tag{3.66}$$

Here ϕ_j^u, ϕ_j^v, and ϕ_j^w are known functions of position, n represents the number of terms in the approximation for the displacement components, and a_j, b_j, and d_j are constants determined by requiring that each of the variational statements holds for arbitrary variations of u, v, and w. This latter requirement is equivalent to the weak form holding for arbitrary variations of a, b, and d. The approximation functions for the displacement components in each direction are selected as power series in terms of the coordinate variables x,y, and z (e.g. 1, x, y, z, xy, xz, yz, x^2, y^2, z^2, x^2y, and so on).

Substitution of the approximate displacements and their variations into the variational statement and collecting terms corresponding to the coefficients of the variations of the displacements allows for writing the final equation in matrix form as

$$\begin{bmatrix} [K^{uu}] & [K^{uv}] & [K^{uw}] \\ [K^{vu}] & [K^{vv}] & [K^{vw}] \\ [K^{wu}] & [K^{wv}] & [K^{ww}] \end{bmatrix} \begin{Bmatrix} \{a\} \\ \{b\} \\ \{d\} \end{Bmatrix} - \tag{3.67}$$

$$\omega^2 \begin{bmatrix} [M^{uu}] & [0] & [0] \\ [0] & [M^{vv}] & [0] \\ [0] & [0] & [M^{ww}] \end{bmatrix} \begin{Bmatrix} \{a\} \\ \{b\} \\ \{d\} \end{Bmatrix} = \begin{Bmatrix} \{0\} \\ \{0\} \\ \{0\} \end{Bmatrix}$$

By using a conventional solution technique, this system of equations can be solved for the natural frequencies of the solid. Results obtained using this method have been compared with other solutions, with excellent accuracy being obtained [24-26].

The explicit form of the elements of each of the sub-matrices in Equations 3.64, $[K]$ and $[M]$, are given below before substitution of the specific approximations functions for the components of the displacements.

$$K_{ij}^{uu} = \int_V \left(C_{11} \frac{\partial \phi_i^u}{\partial x} \frac{\partial \phi_j^u}{\partial x} + C_{66} \frac{\partial \phi_i^u}{\partial y} \frac{\partial \phi_j^u}{\partial y} + C_{55} \frac{\partial \phi_i^u}{\partial z} \frac{\partial \phi_j^u}{\partial z} \right) dV \tag{3.68}$$

$$K_{ij}^{uv} = \int_V \left(C_{12} \frac{\partial \phi_i^u}{\partial x} \frac{\partial \phi_j^v}{\partial y} + C_{66} \frac{\partial \phi_i^u}{\partial y} \frac{\partial \phi_j^v}{\partial x} \right) dV \tag{3.69}$$

$$K_{ij}^{uw} = \int_V \left(C_{13} \frac{\partial \phi_i^u}{\partial x} \frac{\partial \phi_j^w}{\partial z} + C_{55} \frac{\partial \phi_i^u}{\partial z} \frac{\partial \phi_j^w}{\partial x} \right) dV \tag{3.70}$$

$$K_{ij}^{vv} = \int_V \left(C_{66} \frac{\partial \phi_i^v}{\partial x} \frac{\partial \phi_j^v}{\partial x} + C_{22} \frac{\partial \phi_i^v}{\partial y} \frac{\partial \phi_j^v}{\partial y} + C_{44} \frac{\partial \phi_i^v}{\partial z} \frac{\partial \phi_j^v}{\partial z} \right) dV \tag{3.71}$$

$$K_{ij}^{vw} = \int_V \left(C_{23} \frac{\partial \phi_i^v}{\partial z} \frac{\partial \phi_j^w}{\partial z} + C_{44} \frac{\partial \phi_i^v}{\partial z} \frac{\partial \phi_j^w}{\partial y} \right) dV \tag{3.72}$$

$$K_{ij}^{ww} = \int_V \left(C_{55} \frac{\partial \phi_i^w}{\partial x} \frac{\partial \phi_j^w}{\partial x} + C_{44} \frac{\partial \phi_i^w}{\partial y} \frac{\partial \phi_j^w}{\partial y} + C_{33} \frac{\partial \phi_i^w}{\partial z} \frac{\partial \phi_j^w}{\partial z} \right) dV \tag{3.73}$$

$$M_{ij}^{uu} = \int_V \rho \phi_i^u \phi_j^u dV \tag{3.74}$$

$$M_{ij}^{vv} = \int_V \rho \phi_i^v \phi_j^v dV \tag{3.75}$$

$$M_{ij}^{ww} = \int_V \rho \phi_i^w \phi_j^w dV \tag{3.76}$$

The mass and stiffness matrices given by Equations 3.68-3.76 are assembled for particles, with different shapes and made of different materials, within a Fortran program written by the author. The vibrational spectra of these particles are then evaluated using standard eigenvalue solvers.

The three methods used in this study to evaluate the vibrational spectra of nanoparticles with different sizes, shapes, and made of different materials have been

presented. All these methods resulted in general eigenvalue problems which solutions provide the natural frequencies and corresponding mode shapes for the particles considered. Although the final equations to be solve for all the presented methods have the same form, their components are different.

The molecular mechanics method resulted in a diagonal mass matrix which elements are the masses of each individual atom forming the nanostructure. The resulting mass matrix in the molecular dynamics approach is also diagonal, but its components are obtained by multiplying the mass density of the continuum material by the volume of a cube with side equal to the lattice constant. In the continuum mechanics method, a consistent mass matrix is obtained, that is, the mass is distributed over the volume of the solid according to the approximation functions used for the displacements.

The stiffness matrices are also different for each method. For the molecular mechanics method, the stiffness matrix represents the interactions among particles at the atomic scale. The molecular dynamics model resulted in a stiffness matrix that describes the interaction among mass points, and their elements are stated in terms of the components of the continuum elastic tensor. The continuum mechanics stiffness matrix is also a function of the elasticity tensor, and its components basically represent the elastic strain energy stored in the solid when undergoes deformation.

In summary, the molecular mechanics approach describes the vibrational behavior of the particles at the atomic scale, and it can be used to evaluate the variation of the particle properties with the number of atoms forming the nanostructure. For the molecular dynamics approach, the mass and stiffness matrices are evaluated in terms

of the material continuum properties. Therefore, the molecular dynamics method is more a "quasi-continuum approach" rather than a "molecular approach". The continuum mechanics method is based on the classic theory of elasticity, and its applicability for the calculation of the natural frequencies of particles as their size tends towards the nanoscale is evaluated by comparing the calculated frequencies with those obtained using molecular mechanics.

Natural frequencies and modes shapes evaluated using all the methods presented here are listed, discussed, and compared in the next chapter.

Chapter 4
Numerical Applications

In this chapter, the calculated natural vibrational frequencies of isotropic and cubic nanostructures using the three methods introduced in Chapter 3 (molecular mechanics, molecular dynamics, and continuum mechanics) are presented.

Three different materials are considered in this work. They are silicon (Si), germanium (Ge), and carbon (C). The components of the elastic stiffness tensor, and the mass density for each of these materials are presented in Table 4.1 for the case of cubic material symmetry [29]. The elastic stiffness constants for the case of isotropic behavior are shown in Table 4.2. They where obtained based on those for cubic behavior as follows: $C_{11}^I = 2C_{44}^C + C_{12}^C$, $C_{12}^I = C_{12}^C$, and $C_{44}^I = C_{44}^C$, where the superscripts I and C indicate isotropic and cubic behavior, respectively. The properties listed in Tables 4.1 and 4.2 are referred to a coordinate system which orientation relative to the crystal structure is shown in Figure 4.1.

Table 4.1 Material Properties - Cubic Behavior

Material	**Density (g/cm^3)**	**C$_{11}$ (MPa)**	**C$_{12}$ (MPa)**	**C$_{44}$ (MPa)**
Silicon	2.329	166.0	63.9	79.6
Germanium	5.323	128.9	48.3	67.1
Carbon	3.515	1079.0	124.0	578.0

Nanoparticles having four different geometries were considered: spheres, cubes, tetrahedrons, and pyramids. The orientation of the different geometries relative to the Cartesian coordinate system in which they are described is crucial when considering materials having anisotropic behavior. It should match not only the orientation in

Table 4.2 Material Properties - Isotropic Behavior

Material	**Density (g/cm^3)**	**C_{11} (MPa)**	**C_{12} (MPa)**	**C_{44} (MPa)**
Silicon	2.329	223.1	63.9	79.6
Germanium	5.323	182.5	48.3	67.1
Carbon	3.515	1280.0	124.0	578.0

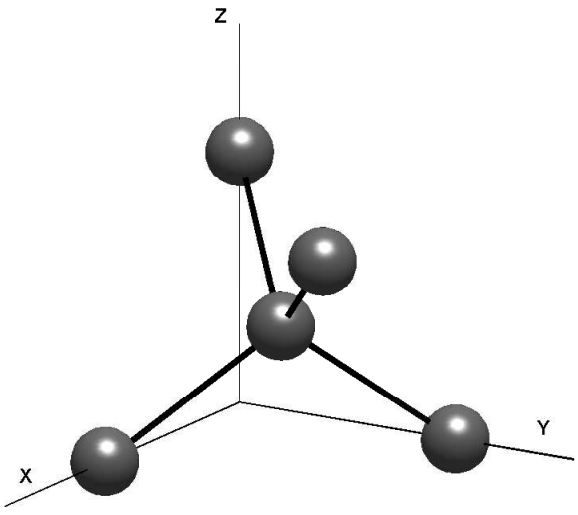

Figure 4.1 Orientation of the cubic crystal structure.

which the elastic constants were determined, but also the crystal orientation used in the atomistic model. Spherical nanoparticles of radius R where defined with the center located at the origin of the coordinate system and with arbitrary orientation of the (x,y,z) axes. Cubes with side length L were considered with the origin located at one of the corners with the axes parallel to the sides. Tetrahedrons with edge length a had the origin of the coordinate system located at one the tips of the solid, and they are oriented such that the z-axis coincides with the height and the x-axis is parallel to on the sides of the triangle forming the base of the tetrahedron. For the pyramids, the origin of the coordinate system is located at the apex, with the z-axis along the height, and with the x- and y-axes parallel to the sides of the square forming the base of the pyramid. These orientations and locations of the Cartesian coordinate systems were used in the continuum mechanics analyses, and they are shown in Figure 4.2 for each of the different geometries. Note that the coordinate system for the tetrahedron does not coincide with that of the crystal (Figure 4.1). As a consequence, the elastic stiffness tensor was transformed in order to have their components defined in such a way to be consistent with the crystal orientation used in the molecular mechanics computations.

The natural frequencies reported in Tables 4.6 to 4.20 have been normalized as

$$\eta = \frac{\omega R}{C_t} \tag{4.1}$$

where η represents the normalized frequencies, ω are the frequencies obtained from the analyses, $C_t = \sqrt{C_{44}/\rho}$ is the shear wave speed, and R is the radius of the sphere for the case of spherical nanoparticles. For the other geometries, R is the radius of a

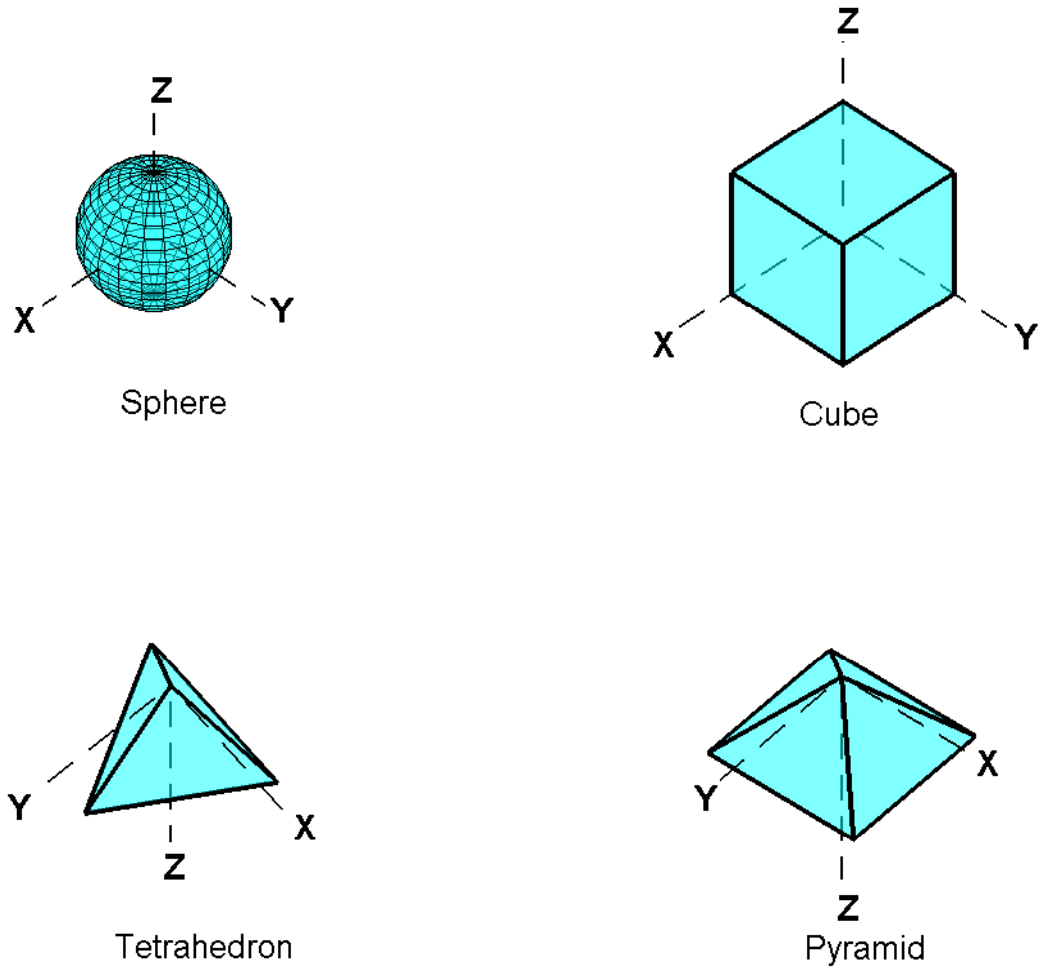

Figure 4.2 Shapes of nanostructures.

sphere having the same volume as that of the corresponding shape. For the case of cube-shaped nanoparticles, $L = 1.6119915R$ with L being the side length of the cube. For tetrahedron-shaped solids, $a = 3.287896694R$ with a being the edge length of the tetrahedron. For pyramid-shaped particles, $h = 1.46459R$ with h being the height of the pyramid with sloped faces at an angle of 45 degrees (i.e. the length of the square base is twice the height of the pyramid).

Molecular mechanics was used to determine the natural frequencies of sphere-, cube-, and tetrahedron-shaped nanoparticles. Pyramid-shaped nanostructures were not analyzed using this approach because this is not a shape that the materials considered in this study would naturally form at the nanoscale level due to their crystal geometric structures. On the other hand, the natural frequencies of sphere-, cube-, and pyramid-shaped silicon nanoparticles having isotropic and cubic symmetries were calculated using molecular dynamics, but tetrahedron-shaped nanostructures were not considered because the molecular dynamics approach employed here is based on a cubic lattice with which is not possible to reproduce all the geometric symmetries of a tetrahedron. The continuum approach can model all shapes and material symmetries.

The remainder of this Chapter is divided into three sections: first, the results obtained using the molecular mechanics and continuum mechanics models are presented, discussed, and compared. Those obtained using the molecular dynamics approach are presented in the second section, along with the results obtained from continuum mechanics for comparison. In the final section of this Chapter a brief discussion of the vibrational behavior of nanostructures according to the reported results is presented.

4.1 Molecular Mechanics

In order to study the size dependence of the natural frequencies, nanostructures having different dimensions and a differing number of atoms were studied. These are presented in Tables 4.3, 4.4,and 4.5 for the cases of the spheres, cubes, and tetrahedrons respectively. These values will of course be non-dimensionalized as discussed in a previous section.

Table 4.3 Radius R, in $\mathring{A}$, of the sphere-shaped nanoparticles considered in the molecular mechanics approach

Atoms	**123**	**227**	**477**	**933**
Silicon	7.3280	9.2000	12.8463	15.6620
Germanium	7.6869	9.6155	13.4122	16.3476
Carbon	4.8671	6.1317	8.5297	10.3863

Table 4.4 Side length L, in $\mathring{A}$, of the cube-shaped nanoparticles considered in the molecular mechanics approach

Atoms	**64**	**216**	**512**	**1000**
Silicon	9.5656	14.9988	20.4356	25.8838
Germanium	9.9925	15.6652	21.3273	26.9892
Carbon	6.3597	9.9605	13.5840	17.1774

Table 4.5 Edge length a, in $\mathring{A}$, of the tetrahedron-shaped nanoparticles considered in the molecular mechanics approach

Atoms	**51**	**136**	**281**	**502**	**815**
Silicon	11.5125	19.1960	26.8761	34.5539	42.2301
Germanium	12.0154	20.0380	28.0560	36.0709	44.0838
Carbon	7.5635	12.6377	17.7171	22.7996	27.8841

The maximum number of atoms considered for each of the particles studied was

limited by the capabilities of the molecular mechanics software used for the calculations, and the computational time required to run the simulations.

4.1.1 Sphere-Shaped Nanostructures

The lowest 20 normalized natural frequencies obtained for spherical nanoparticles along with those obtained from continuum mechanics are listed in Tables 4.6, 4.7, and 4.8 for silicon, germanium, and carbon structures.

Results indicate that there is in fact a dependence on the nanostructure size of the vibrational frequencies at the nanoscale, not only the magnitude of the normalized frequencies changes, but also the number and location of the degenerate modes.

The magnitude of the normalized frequencies increases as the size of the particles is increased. For silicon, some of the frequencies remain below and others surpass the values obtained from continuum mechanics, with the maximum difference being about $\pm$ 7.0% compared to the frequencies calculated for the case in which cubic symmetry was assumed. For germanium, all the frequencies are consistently lower than those from continuum mechanics for the case of isotropic symmetry, while they are higher than those obtained for the cubic case, with differences ranging from about 16% to 28%. Normalized frequencies for carbon nanoparticles are all lower than the continuum values, being between 6% and 17% below those for the case of cubic behavior.

The behavior of the lowest frequency as a function of the number of atoms forming the particles, and as a function of the radius of the sphere is illustrated in Figures 4.3 and 4.4, respectively. It is interesting to see that the global behavior of the particles for the three materials considered is similar. However, it is clear that there is not

a smooth variation with number of atoms or radius, and it is not possible to fit an acceptable equation to describe the size dependence of the natural frequencies. This behavior may be caused by the variation of the geometry of the spherical particles with the number of atoms. The geometry of the molecular structures modeled using molecular mechanics is not perfectly spherical, and their geometric shape changes as the number of atoms is increased as shown in Figure 4.5, with the molecule formed by the highest number atoms being the one with a geometry closest to a sphere. The reported radii were calculated as the average of the maximum and minimum values. These values correspond to the largest and smallest distances between pair of atoms located at the surface of the different sphere-shaped nanoparticles.

Somewhat surprisingly, the lower mode shapes of silicon spheres formed by 933 atoms are practically identical for both molecular and continuum mechanics approaches. The only difference is provided by the fact that the mode shape corresponding to the 8^{th} molecular frequency matches the mode shape associated with the 14^{th} continuum frequency. The modes shapes corresponding to the first four degenerate groups are shown in Figures 4.6 and 4.7. It is recommended to view the animated versions which are available at the web site: www.engr.colostate.edu\~framirez following, the link Nanoparticle Vibrations.

4.1.2 Cube-Shaped Nanostructures

Tables 4.9, 4.10, and 4.11 contain the lowest 20 normalized frequencies for silicon, germanium, and carbon cube-shaped nanoparticles respectively, calculated with molecular and continuum mechanics for cubic and isotropic material symmetry.

Once again the frequency size dependence is exhibited. The number and location

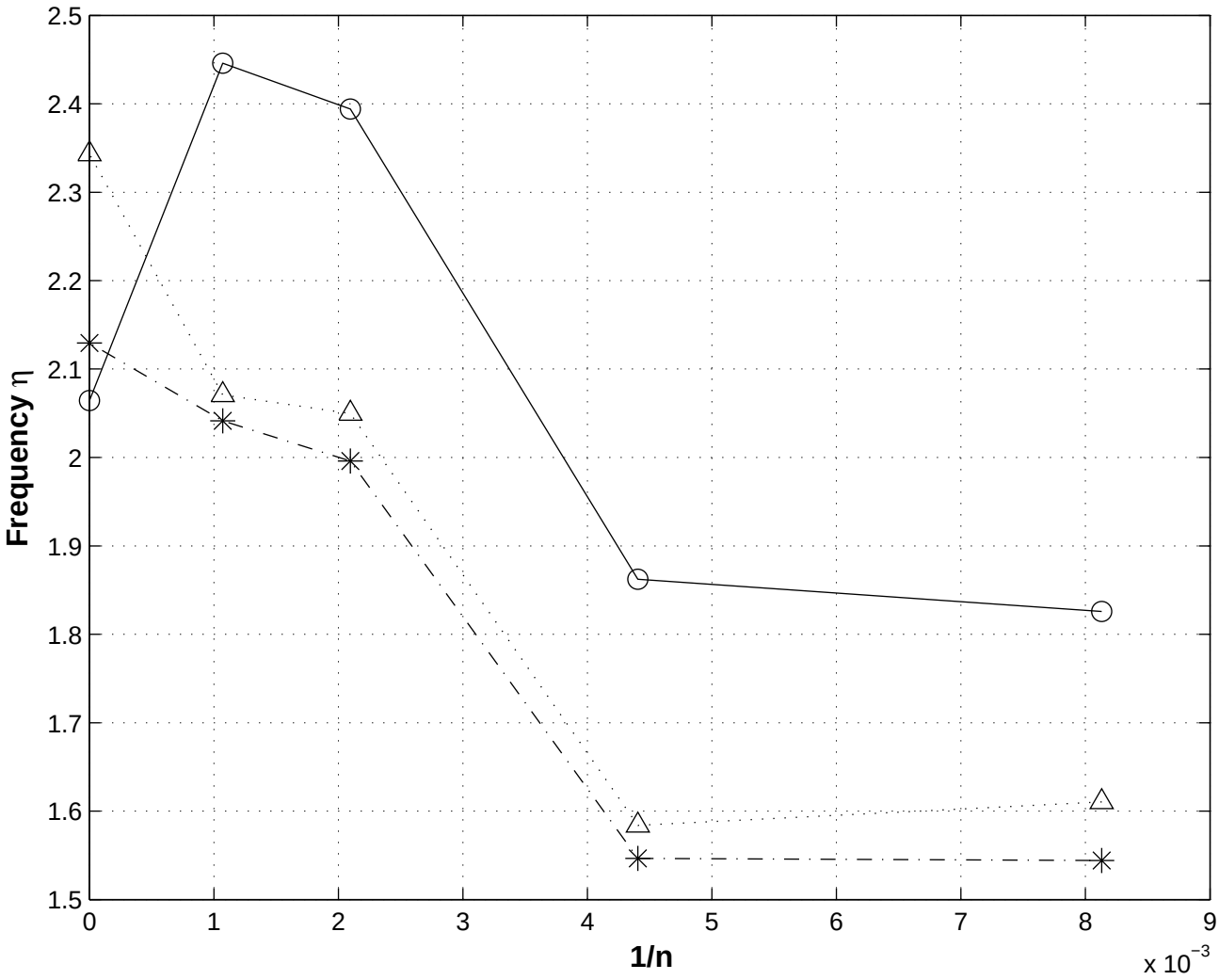

Figure 4.3 Lowest normalized natural frequency for silicon (∗), germanium (○), and carbon (△) sphere-shaped nanostructures as function of the number of atoms (n). Frequencies at 1/n=0 correspond to continuum mechanics results for cubic material symmetry.

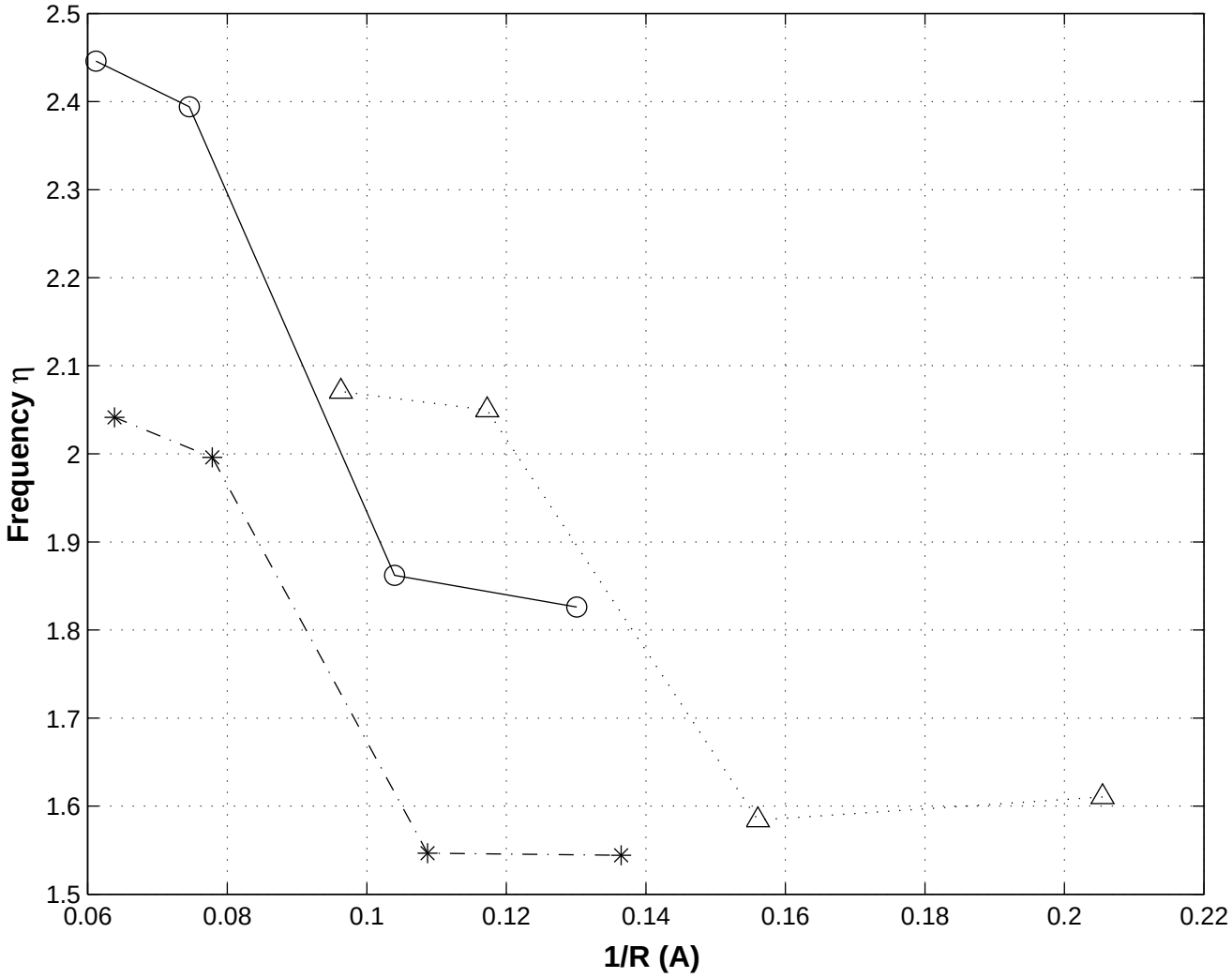

Figure 4.4 Lowest normalized natural frequency for silicon (∗), germanium (○), and carbon (△) sphere-shaped nanostructures as function of the radius (R).

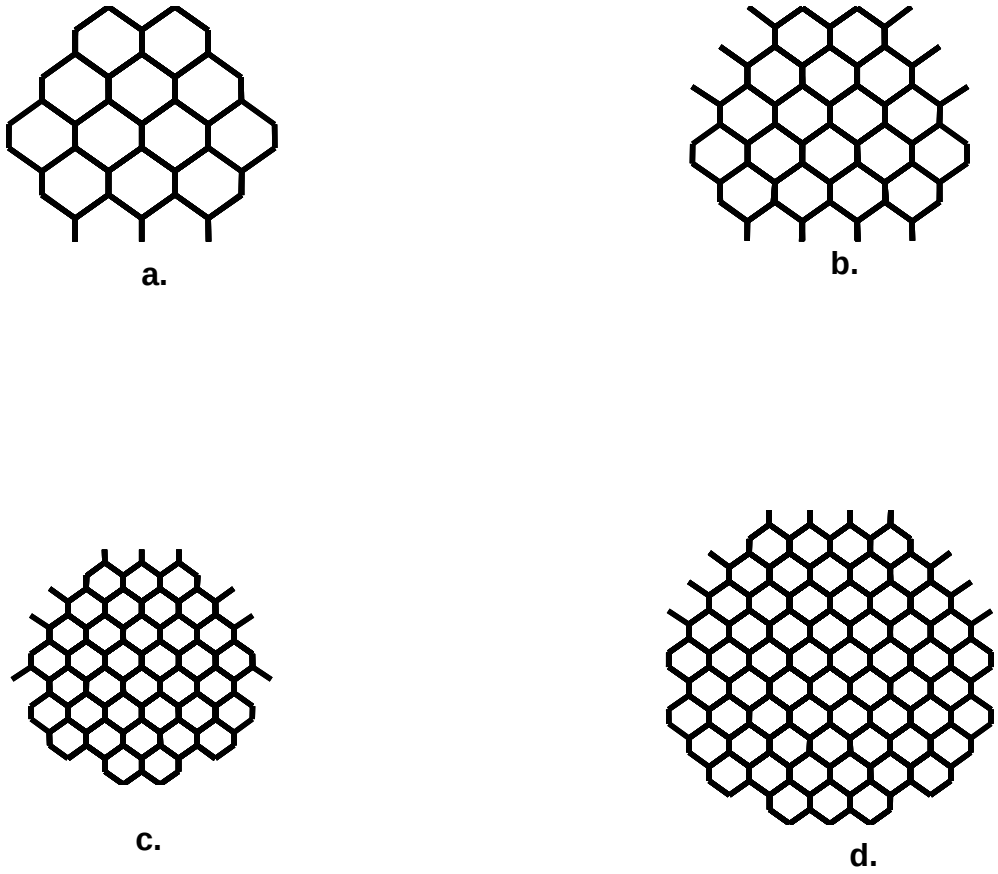

Figure 4.5 Geometry variation of sphere-shaped molecular nanostructures with the number of atoms: a. 123 atoms, b. 227 atoms, c. 477 atoms, and d. 933 atoms (side views).

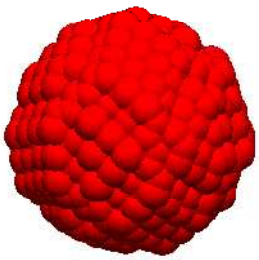

MM: Modes 1, 2, and 3

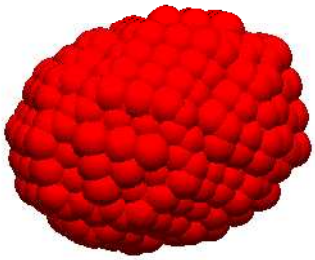

MM: Modes 4, 5, and 6

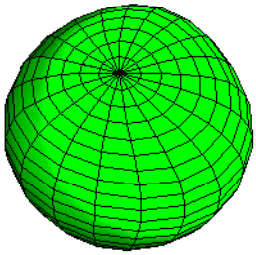

CM: Modes 1, 2, and 3

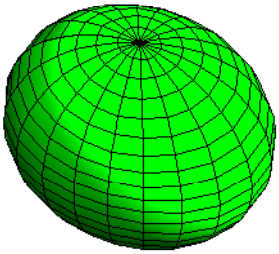

CM: Modes 4, 5, and 6

Figure 4.6 Identical vibrational modes of sphere-shaped nanostructures obtained using molecular mechanics (MM), and continuum mechanics (CM).

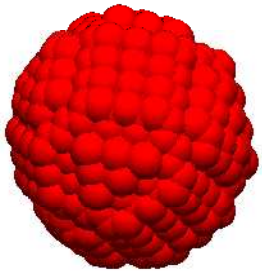

MM: Modes 6 and 7

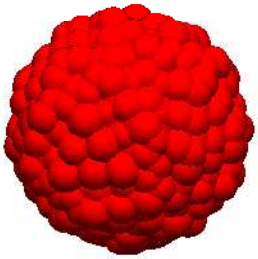

MM: Mode 8

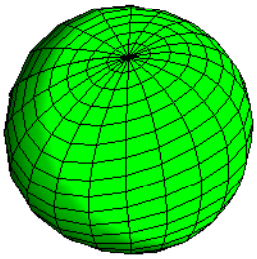

CM: Modes 6 and 7

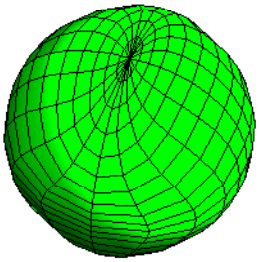

CM: Mode 14

Figure 4.7 Identical vibrational modes of sphere-shaped nanostructures obtained using molecular mechanics (MM), and continuum mechanics (CM).

of the degenerate values also vary, and the magnitude of the normalized frequencies increase with the number of atoms for all materials considered.

Molecular mechanics frequencies of silicon cubes approach the continuum cubic values from below, with differences ranging between 4.4% for the lowest frequency and 13.8% for the 20^{th} frequency. Molecular mechanics analyses result in frequencies higher than the continuum values for germanium cubes when 512 or more atoms are used in the molecular model, with a maximum difference of about 18.4%. For carbon nanoparticles, the frequencies also increase tending to the continuum cubic values from below, with differences between 13.1 and 17.4%.

The behavior of the lowest frequency is illustrated in Figure 4.8 as a function of the number of atoms (n). Once again the variation of the normalized frequency with the number of atoms is similar for all materials considered. This time, the variation is smooth, and second order polynomials were obtained using least square fitting (Figure 4.8). They are given by the following equations for silicon, germanium, and carbon particles respectively.

$$\eta = 3082.35(1/n)^2 - 103.08(1/n) + 1.793 \tag{4.2}$$

$$\eta = 5310.30(1/n)^2 - 156.85(1/n) + 2.22 \tag{4.3}$$

$$\eta = 674.57(1/n)^2 - 41.25(1/n) + 1.50 \tag{4.4}$$

These polynomials result in converged values, i.e. frequencies evaluated at 1/n=0, for the lowest normalized frequency of cube-shaped nanoparticles of 1.793, 2.22, and

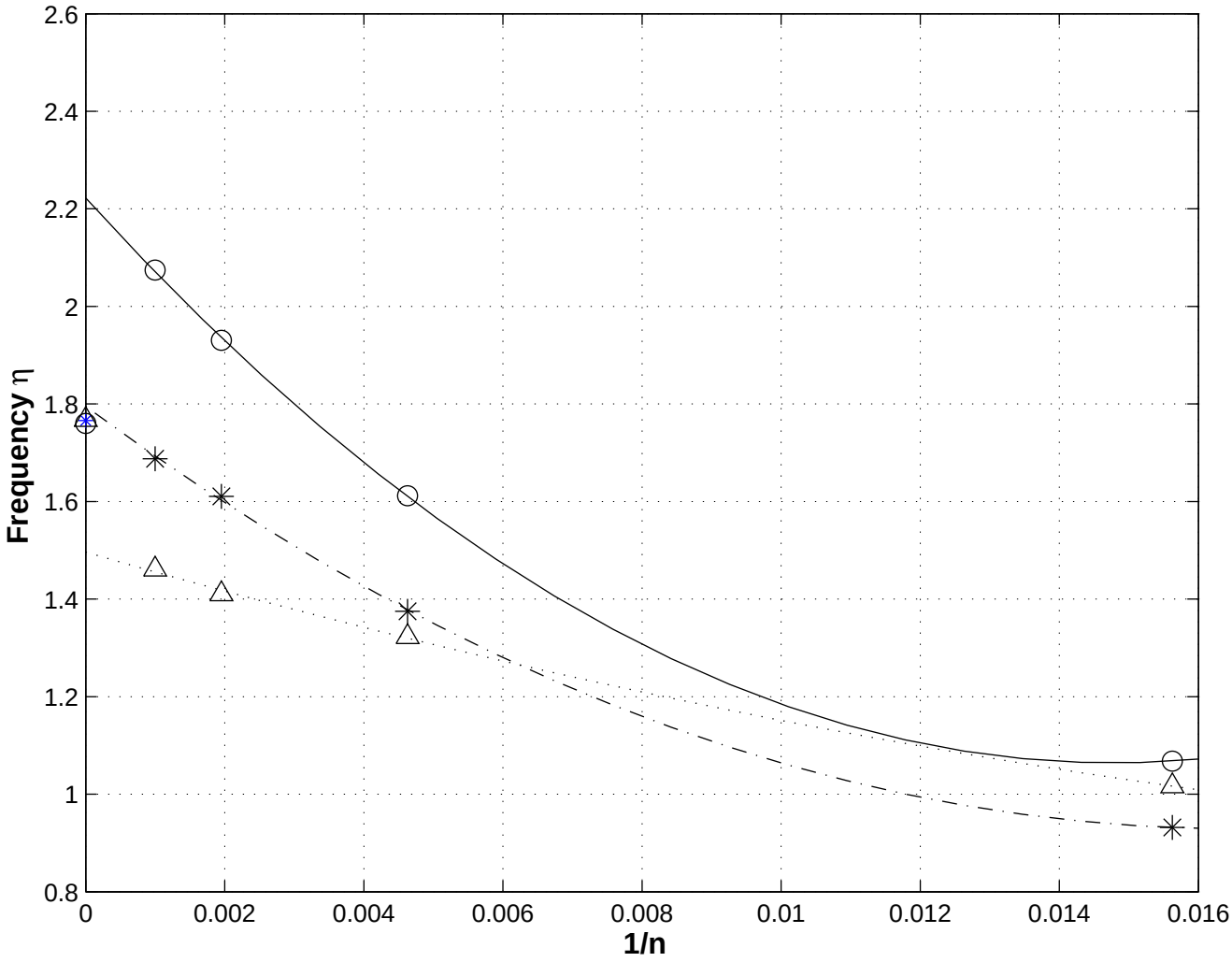

Figure 4.8 Lowest normalized natural frequency for silicon ($*$), germanium ($\circ$), and carbon ($\triangle$) cube-shaped nanostructures as function of the number of atoms (n). Dashed, solid, and dotted lines represent the curve fitting for silicon, germanium, and carbon particles, respectively. Frequencies at 1/n=0 correspond to continuum mechanics results for cubic material symmetry.

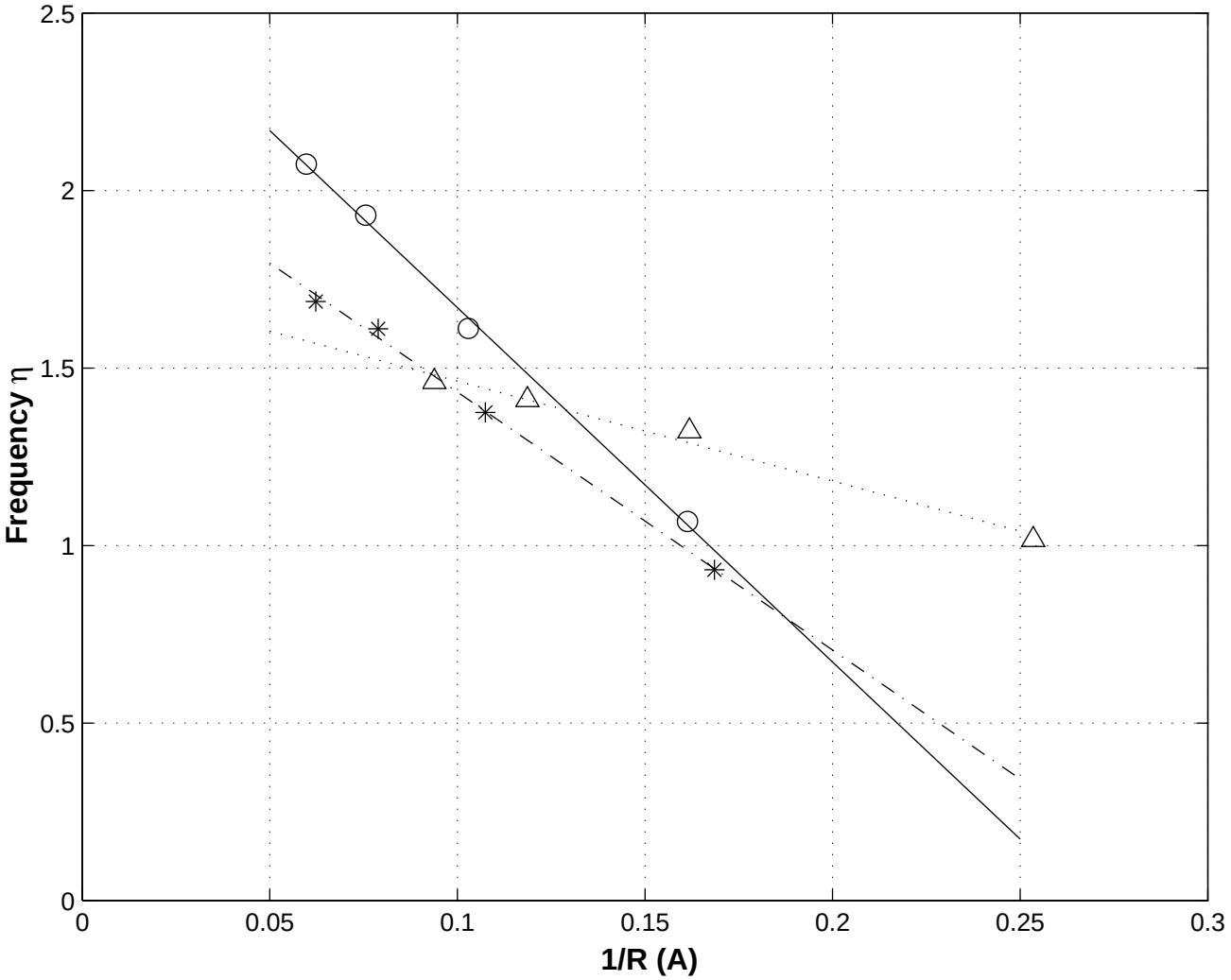

Figure 4.9 Lowest normalized natural frequency for silicon ($*$), germanium ($\circ$), and carbon ($\triangle$) cube-shaped nanostructures as function of the radius (R) of a sphere having the same volume. Dashed, solid, and dotted lines represent the curve fitting for silicon, germanium, and carbon particles, respectively.

1.50 for silicon, germanium, and carbon respectively. Compared with the lowest continuum mechanics frequency obtained assuming cubic symmetry, these values are only 1.8% higher for silicon, 26% higher for germanium, and 15% lower for carbon cubes. There is far better agreement between molecular and continuum mechanics methods for silicon particles than for the other materials.

The poor agreement between molecular and continuum mechanics for germanium and carbon nanoparticles is explained by the fact that the parameters used in the UFF for the interatomic potential of the molecular mechanics method were not determined for vibrational analyses. Force fields are mainly constructed to reproduce structures and energies of molecular structures, and they usually omit fitting vibrational spectroscopy data [27]. There exist various other force fields that have been constructed to fit also vibrational data such as MM3 [28], and the parameters employed in this study may need additional calibration to better represent molecular vibrations.

The variation of the lowest normalized frequency with the size of the particle is illustrated in Figure 4.9 as a function of the radius of an equivalent sphere having the same volume as the corresponding cube-shaped nanoparticle. The variation of the lowest normalized frequency is linear indicating that, for the range of particle sizes considered here, the term ωR is not scale invariant as it is for continuum elasticity. The linear equations representing this behavior were obtained from least-square curve fitting, and they are shown below for silicon, germanium, and carbon cube-shaped nanoparticles, respectively.

$$\eta = -7.269(1/R) + 2.159 \tag{4.5}$$

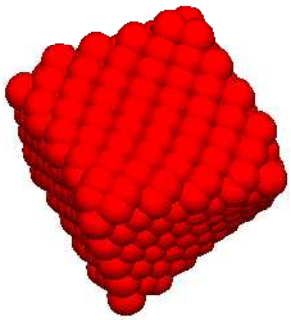

MM: Modes 1 and 2

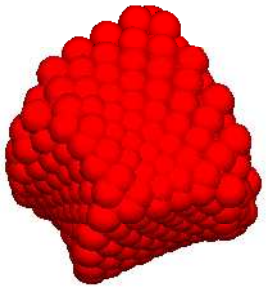

MM: Modes 3 and 4

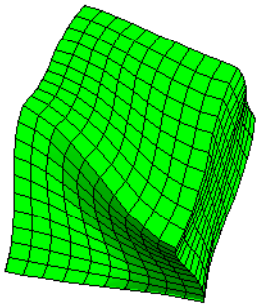

CM: Modes 1 and 2

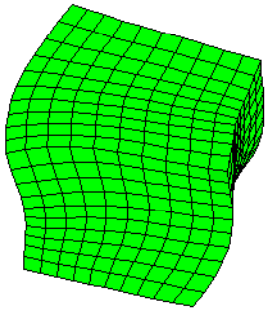

CM: Modes 3 and 4

Figure 4.10 Identical vibrational modes of cube-shaped nanostructures obtained using molecular mechanics (MM), and continuum mechanics (CM).

$$\eta = -9.981(1/R) + 2.668 \tag{4.6}$$

$$\eta = -2.817(1/R) + 1.745 \tag{4.7}$$

In spite of the excellent agreement between the cube geometries modeled for the molecular and continuum mechanics methods, the number and location of the degenerate frequency groups are not the same for these two approaches. However, the mode shapes corresponding to the lowest two frequencies are the same for silicon structures, and some higher modes also have the same deformation although the

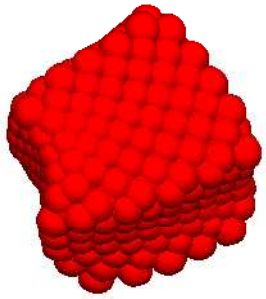

MM: Mode 5

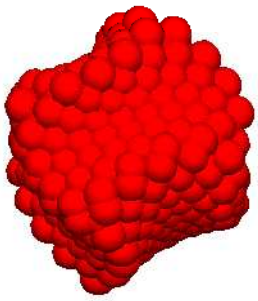

MM: Mode 6

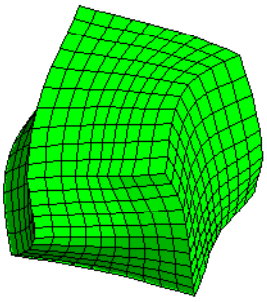

CM: Mode 5

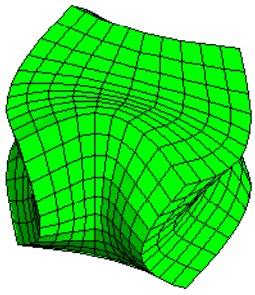

CM: Mode 8

Figure 4.11 Identical vibrational modes of cube-shaped nanostructures obtained using molecular mechanics (MM), and continuum mechanics (CM).

corresponding frequencies appear at different locations. For instance, the molecular mechanics mode shape associated with the sixth lowest frequency is the same as the mode shape associated with the eighth lowest frequency calculated using continuum mechanics. Figures 4.10 and 4.11 illustrate the lowest four degenerate mode shapes for silicon cube-shaped nanoparticles obtained from molecular and continuum mechanics methods.

4.1.3 Tetrahedron-Shaped Nanostructures

It is important to begin this section by noting that the geometry of the molecules used in this approach perfectly describe tetrahedrons which four faces are equilateral triangles. There is no discretization error for this geometry.

The lowest 20 normalized frequencies of silicon, germanium, and carbon tetrahedral particles are shown in Table 4.12, 4.13, and 4.14 respectively, along with the continuum values for isotropic and cubic behaviors. The dependence on the nanostructure size of the frequencies and degenerate modes is confirmed again for all materials, with their magnitudes increasing with the number of atoms forming the molecular model.

Normalized frequencies of silicon and carbon tetrahedrons obtained using molecular mechanics tend toward the continuum values from below. silicon frequencies are between 4.2% and 13.7% lower than continuum values, while the differences for those of carbon range from 13.2% to 18.2%. For germanium tetrahedrons, molecular frequencies are again higher than those obtained using continuum mechanics, with the smallest difference being 3.6% for the 20^{th} frequency and the maximum about 16.9% for the lowest frequency.

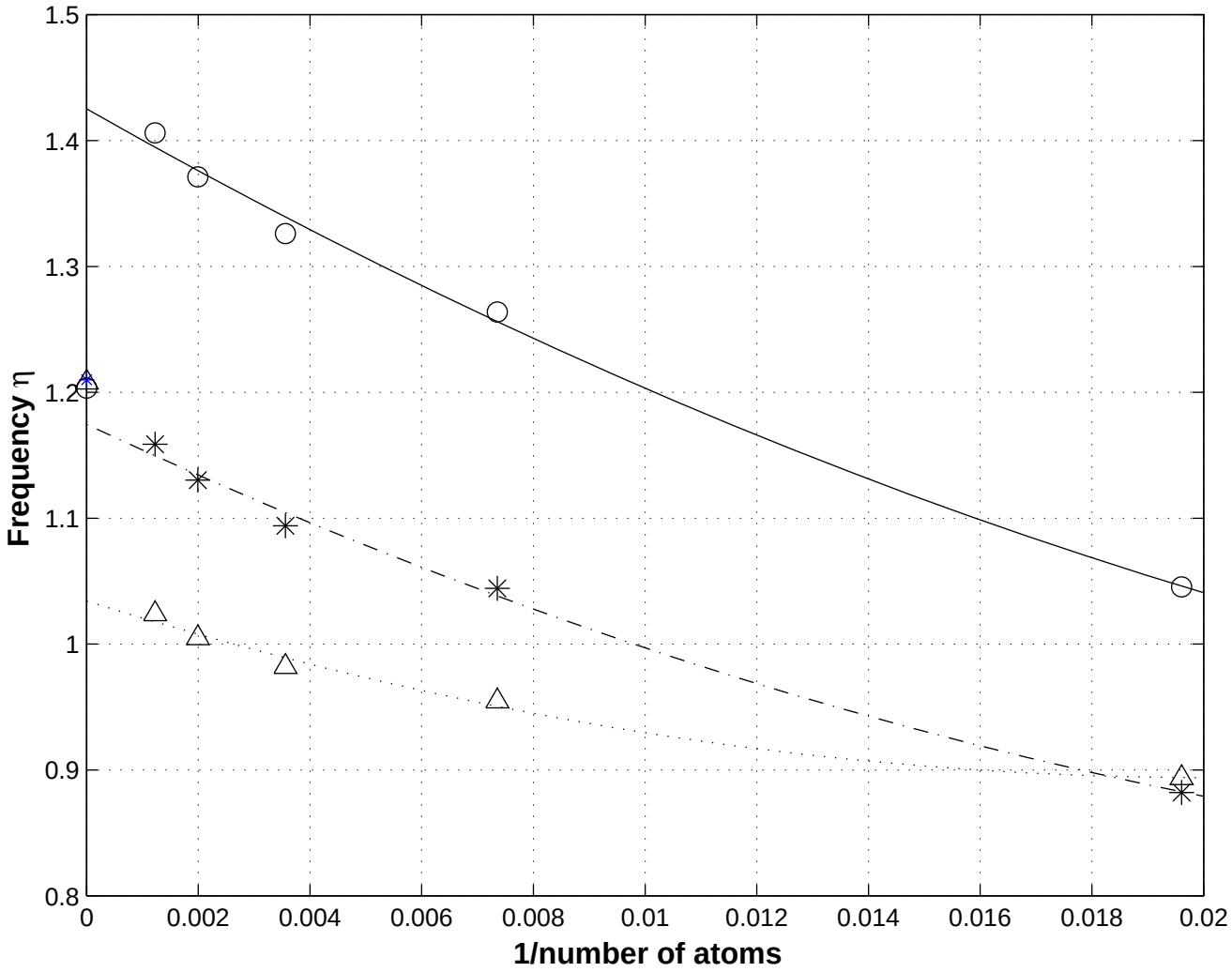

Figure 4.12 Lowest normalized natural frequency for silicon (∗), germanium (○), and carbon (△) tetrahedron-shaped nanostructures as function of the number of atoms (n). Dashed, solid, and dotted lines represent the curve fitting for silicon, germanium, and carbon particles, respectively. Frequencies at 1/n=0 correspond to continuum mechanics results for cubic material symmetry.

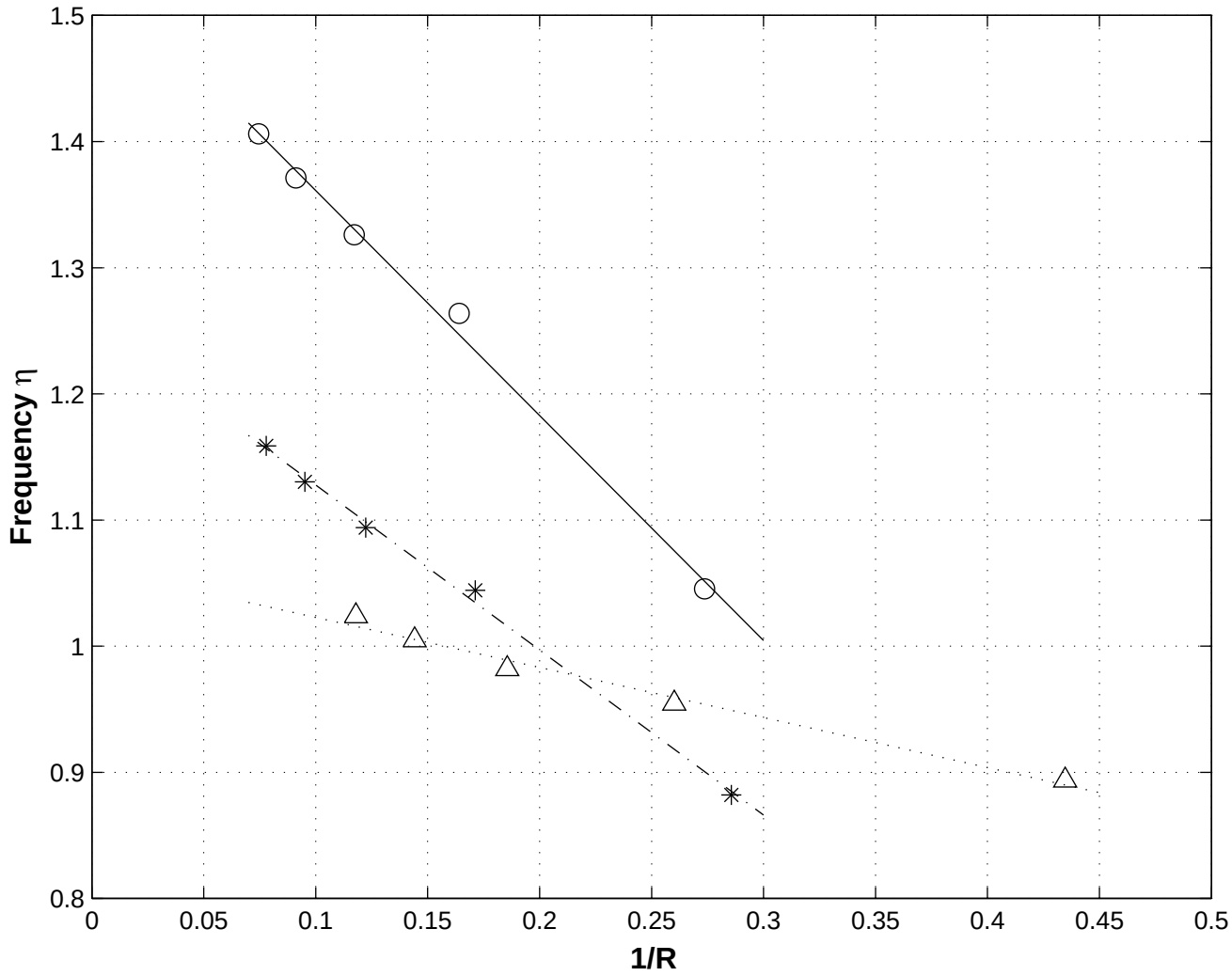

Figure 4.13 Lowest normalized natural frequency for silicon (∗), germanium (○), and carbon (△) tetrahedron-shaped nanostructures as function of the radius (R) of a sphere having the same volume. Dashed, solid, and dotted lines represent the curve fitting for silicon, germanium, and carbon particles, respectively.

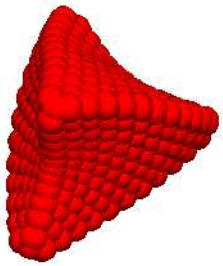

MM: Modes 1 and 2

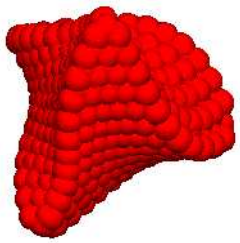

MM: Modes 3, 4, and 5

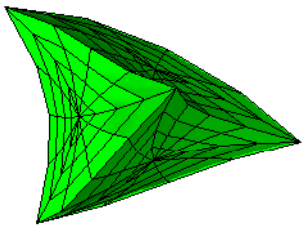

CM: Modes 1 and 2

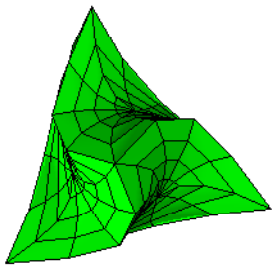

CM: Modes 6, 7 snd 8

Figure 4.14 Identical vibrational modes of tetrahedron-shaped nanostructures obtained using molecular mechanics (MM), and continuum mechanics (CM).

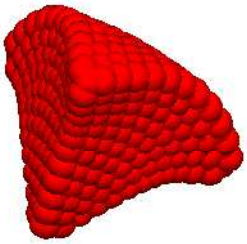

MM: Modes 6, 7, and 8

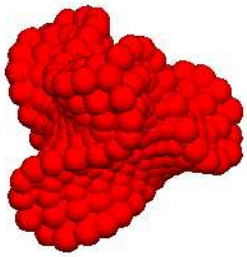

MM: Mode 9

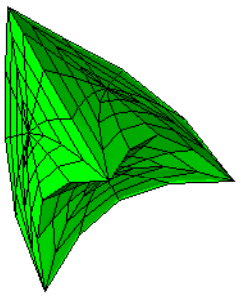

CM: Modes 3, 4 and 5

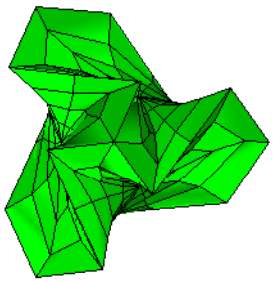

CM: Mode 9

Figure 4.15 Identical vibrational modes of tetrahedron-shaped nanostructures obtained using molecular mechanics (MM), and continuum mechanics (CM).

The behavior of the lowest frequency with the number of atoms in the molecular mechanics model is similar for silicon, germanium, and carbon particles as shown in Figure 4.12. The exhibited smooth variation allows the fitting of second order polynomials, which are presented in Equations 4.5, 4.6, and 4.7 for silicon, germanium, and carbon respectively.

$$\eta = 301.08(1/n)^2 - 20.81(1/n) + 1.175 \tag{4.8}$$

$$\eta = 2972.15(1/n)^2 - 48.40(1/n) + 1.46 \tag{4.9}$$

$$\eta = 344.81(1/n)^2 - 13.92(1/n) + 1.04 \tag{4.10}$$

According to these polynomials, the converged value for silicon tetrahedrons is 1.175 which is only 2.9% lower than the continuum value. For germanium and carbon particles, these equations indicate that converged values for the lowest frequency are 1.46 and 1.04, which are 21.3% higher, and 13.9% lower than those obtained using continuum mechanics.

The variation of the lowest normalized frequency with the size of the particle is illustrated in Figure 4.13 as a function of the radius of an equivalent sphere having the same volume as the corresponding tetrahedron-shaped nanoparticle. The variation of the lowest normalized frequency is again linear indicating that the scale invariance of the term ωR holding for continuum elasticity, does not hold for the range of sizes studied here. The linear equations representing this behavior were obtained from

least-square curve fitting, and they are shown below for silicon, germanium, and carbon cube-shaped nanoparticles, respectively.

$$\eta = -1.308(1/R) + 1.259 \tag{4.11}$$

$$\eta = -1.784(1/R) + 1.539 \tag{4.12}$$

$$\eta = -0.397(1/R) + 1.063 \tag{4.13}$$

The number and groups of degenerate frequencies match for both, molecular and continuum mechanics methods. The mode shapes are also the same as illustrated in Figures 4.14 and 4.15 for silicon tetrahedrons.

4.2 Molecular Dynamics

The molecular dynamics model presented in Chapter 3 was employed to calculate the natural vibrational frequencies of sphere-, cube-, and pyramid-shaped silicon structures with radius, side length, and height of 10.0, 16.119915, and 14.6459 $\mathring{A}$ respectively. The accuracy and convergence of this method was studied by analyzing solids discretized into an increasing number of mass points (m). For spheres 312, 624, 1064, 1640, 2368, and 7736 mass points were considered, cubes were discretized into 343, 729, 1331, 2197, and 8000 points, while 406, 904, 1690, and 6416 were used for the pyramids.

4.2.1 Sphere-Shaped Nanostructures

The lowest 20 normalized frequencies determined using this method, as well as those obtained from continuum mechanics are reported in Table 4.15 for the isotropic case, and in Table 4.16 for the case in which cubic symmetry was considered.

The magnitude of the normalized frequencies increases as the number of mass points (m) comprising the solid is increased for both material symmetries considered, and they tend towards the continuum values with a maximum difference of about 12%. The number and location of the degenerate frequencies are the same for these two methods as expected, this behavior is explained by the fact that the potential energy constants used in the molecular dynamics approach were determined to represent the components of the continuum elastic stiffness tensor.

The variation of the lowest frequency with the number of mass points is illustrated in Figures 4.16 and 4.17 along with curves obtained using least squares polynomial fitting. Equations 4.8 and 4.9 show the obtained second order polynomials, and they indicate converged values of 2.24 and 1.92 for the isotropic and cubic cases respectively, these normalized frequencies are about 10% lower than those obtained from continuum mechanics.

$$\eta = 49455.56(1/m)^2 - 318.31(1/m) + 2.24 \tag{4.14}$$

$$\eta = 51552.14(1/m)^2 - 297.71(1/m) + 1.92 \tag{4.15}$$

Murray [30] and co-workers used the present molecular dynamics method to evalu-

ate the natural vibration frequencies of isotropic spheres, and they reported excellent agreement with exact solutions, with differences smaller than 1%. Their calculation of the frequencies is done by giving an initial velocity or strain to the lattice structure, and the subsequent motion is simulated. The motion of individual atoms are then Fourier analized to yield the spectrum of vibrational frequencies. The excellent agreement between molecular dynamics and exact solutions reported by Murray was not achieved in the present study. Some of the possible reasons explaining this behavior include the simplifications made here when assuming small amplitude of vibrations as explained in Chapter 3, and another important issue is the number of mass points in which the solids were discretized in this study, which was determined by run time limitations.

4.2.2 Cubed-Shaped Nanostructures

The lowest 20 frequencies for silicon cubes using molecular dynamics are listed in Tables 4.17 and 4.18 for the isotropic and cubic cases respectively. The frequencies of the nanoparticles increase with the number of mass points forming the solid, and they tend towards the continuum values from below with a difference ranging from 5.7 to 8.4%, and from 5.8 and 12.5% for isotropic and cubic behavior respectively. Once again the number and location of the degenerate frequency groups coincide for both molecular dynamics and continuum mechanics methods.

The behavior of the lowest normalized frequency as a function of the number of mass points is illustrated in Figures 4.16 and 4.17. The fitted polynomials are given by Equations 4.10 and 4.11 for the isotropic and cubic cases, resulting in converged frequencies, i.e. evaluated at 1/m=0, of 1.68 and 1.67 which are 5.1% lower than

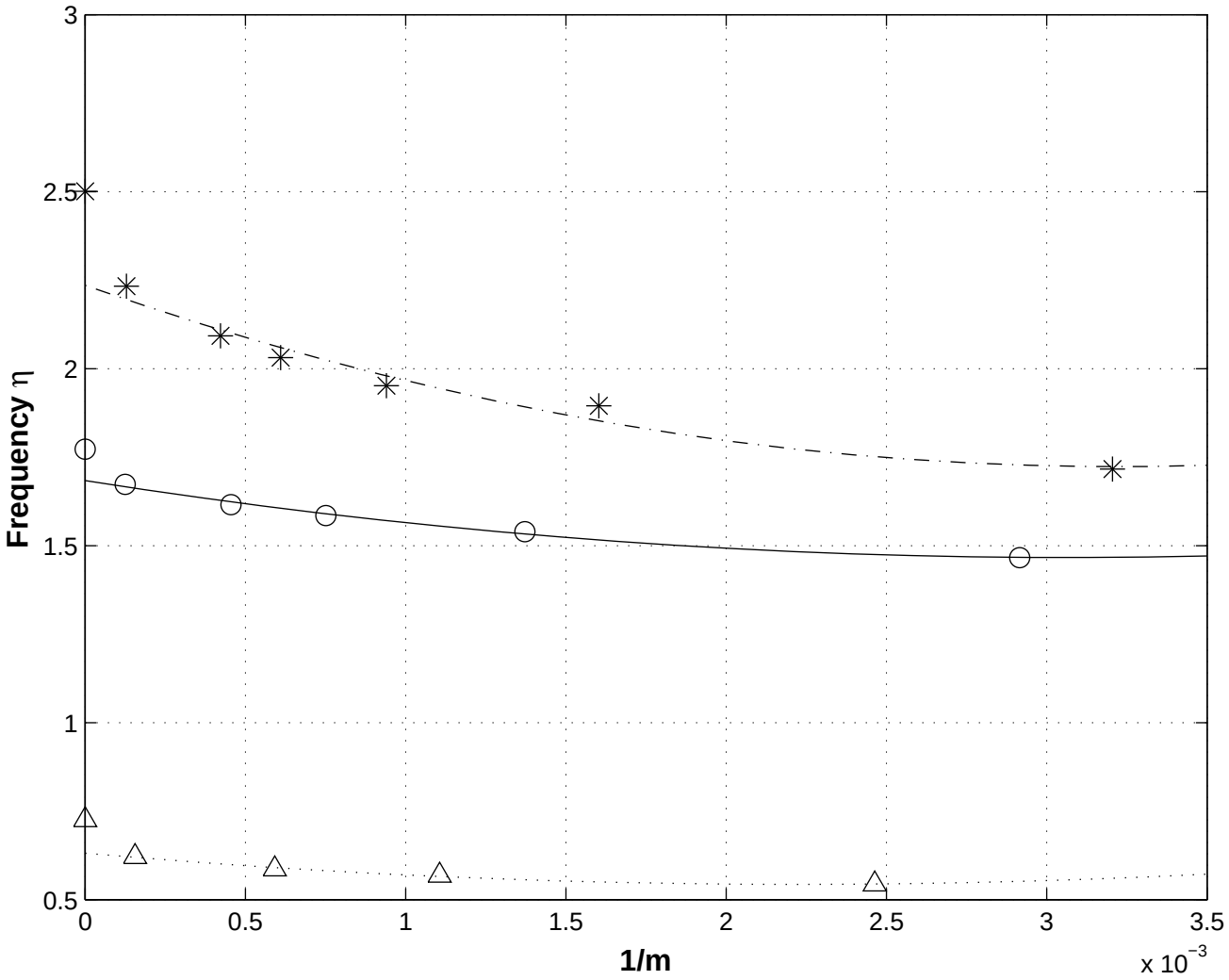

Figure 4.16 Lowest normalized natural frequency of silicon sphere- (∗), cube-(○), and pyramid- (△) shaped nanostructures as function of the number of mass points (m) used in the molecular dynamics model assuming isotropic material symmetry. Dashed, solid, and dotted lines represent the curve fitting for spheres, cubes, and pyramids. Frequencies at 1/ms=0 correspond to continuum mechanics results.

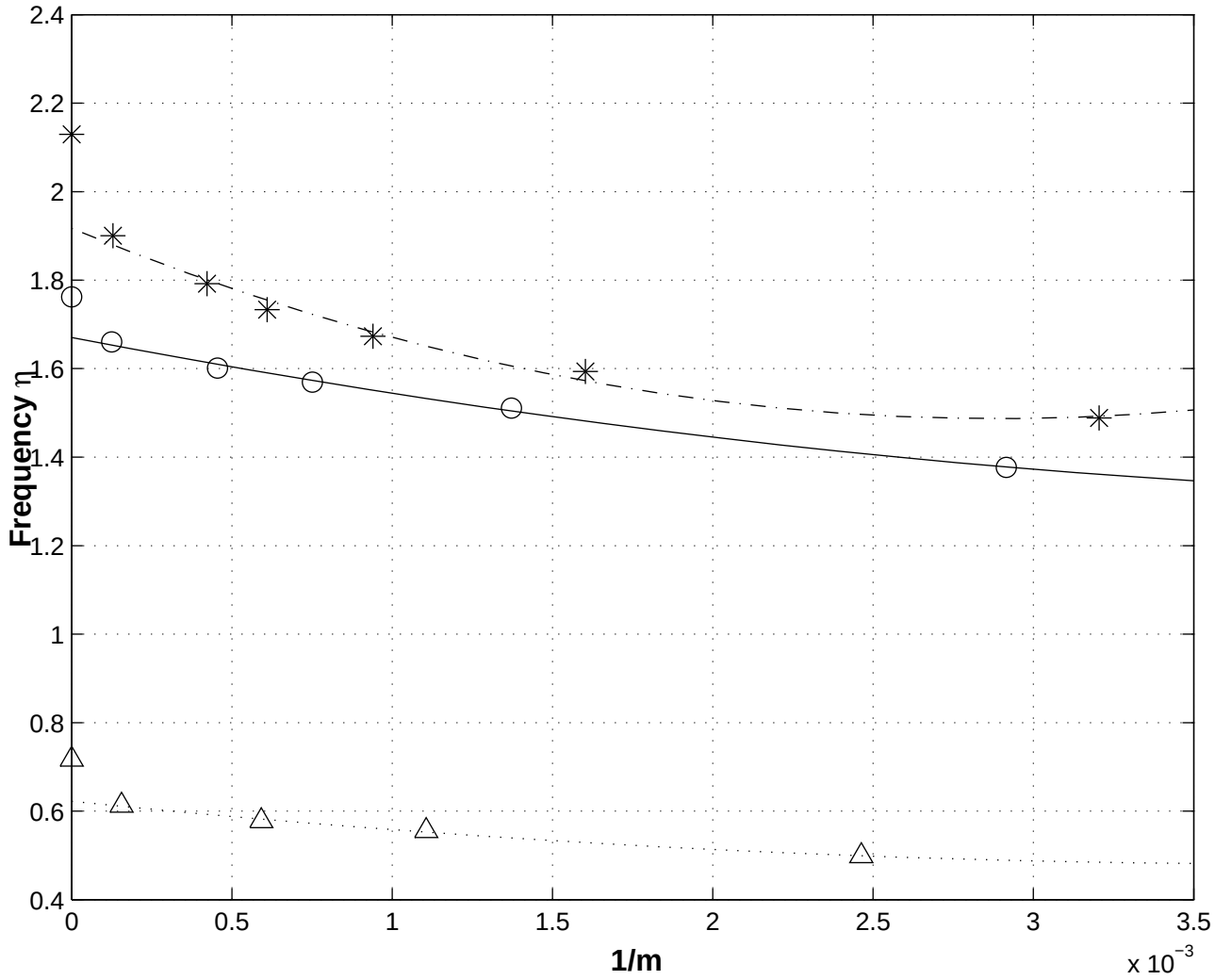

Figure 4.17 Lowest normalized natural frequency of silicon sphere- (∗), cube-(○), and pyramid- (△) shaped nanostructures as function of the number of mass points (m) used in the molecular dynamics model assuming cubic material symmetry. Dashed, solid, and dotted lines represent the curve fitting for spheres, cubes, and pyramids. Frequencies at 1/m=0 correspond to continuum mechanics results.

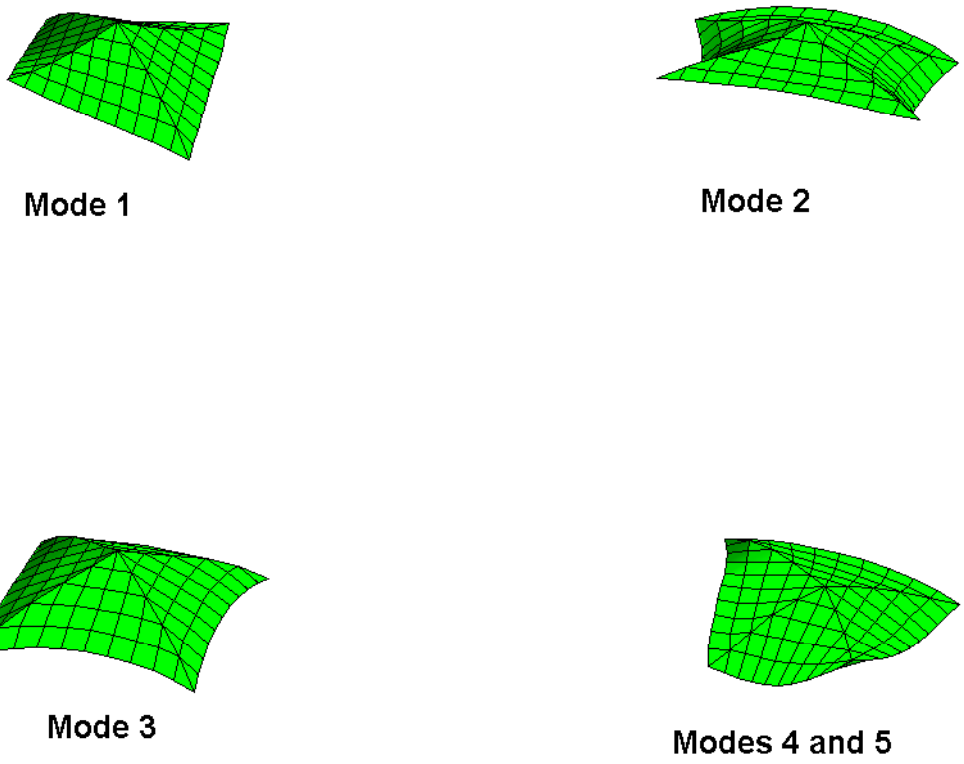

Figure 4.18 Vibrational modes of pyramid-shaped structures obtained using continuum mechanics.

those obtained using continuum mechanics.

$$\eta = 23070.60(1/m)^2 - 141.60(1/m) + 1.68 \tag{4.16}$$

$$\eta = 13385.66(1/m)^2 - 139.38(1/m) + 1.67 \tag{4.17}$$

4.2.3 Pyramid-Shaped Nanostructures

Tables 4.19 and 4.20 report the lowest 20 normalized frequencies obtained using molecular dynamics and continuum mechanics for silicon pyramids assuming isotropic and cubic behavior, respectively.

Once again, the frequencies of the nanoparticles increase as the number of mass points forming the solid is increased, and they approach to the continuum values from

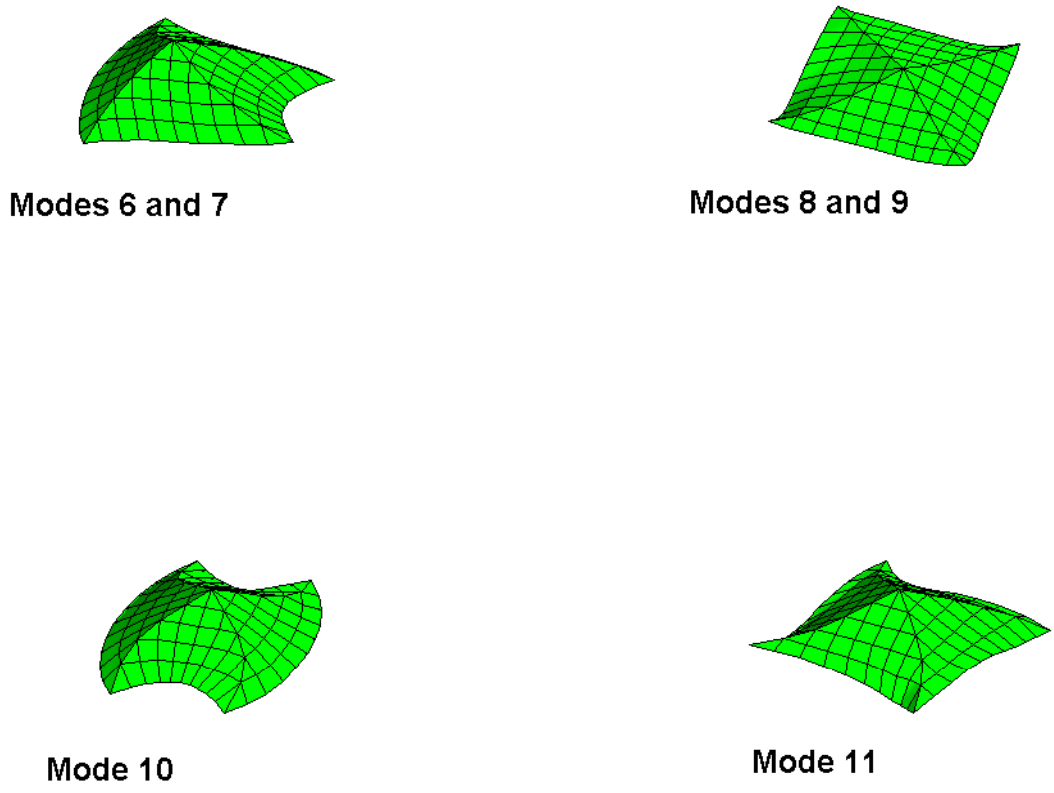

Figure 4.19 Vibrational modes of pyramid-shaped structures obtained using continuum mechanics.

below with differences ranging from 5.7 to 8.4%, and from 5.8 and 12.5% for isotropic and cubic behavior respectively. The variation of the lowest normalized frequency with the number of mass points is illustrated in Figures 4.16 and 4.17. The fitted second order polynomials for the isotropic and cubic cases are given by

$$\eta = 17841.97(1/m)^2 - 79.33(1/m) + 0.63 \tag{4.18}$$

$$\eta = 9530.07(1/m)^2 - 73.49(1/m) + 0.62 \tag{4.19}$$

They indicate that converged values for the lowest frequency are 0.63 and 0.62 for isotropic and cubic symmetries respectively. These values are about 13% lower than those obtained using continuum mechanics.

The number and location of the degenerate frequency groups match for both methods as expected. The mode shapes corresponding to the lowest 8 frequencies are illustrated in Figures 4.18 and 4.19 for the case in which cubic symmetry was assumed.

4.3 Discussion

In this section a summary and discussion of the main features observed based on the results reported in the previous two sections is presented.

Results obtained using the molecular mechanics approach confirmed the size dependence of particles properties at the nanoscale. Not only the magnitude of the natural frequencies, but also the number and location of the degenerate frequency groups change with the number of atoms forming the solid. The magnitude of the

normalized natural frequencies increase nonlinearly with the number of atoms forming the particles. This behavior for the lowest frequency exhibited a smooth variation for the cases of cube- and tetrahedron-shaped nanostructures allowing the fitting of a polynomial to describe this behavior. However, the natural frequencies for sphere-shaped particles was not smooth, and it was not possible to fit an acceptable expression describing their variation with the size of the nanostructures. The latter is attributed to the fact that the geometry of the molecular structures was not perfectly spherical, and it changes with the number of atoms as explained before.

The magnitude of the normalized natural frequencies increase linearly with the size of the nanoparticle. This behavior indicates that the scale invariance of the term ωR in continuum elasticity does not hold for the range of particle sizes considered in this study.

It was observed that the normalized frequencies calculated using the molecular mechanics method, approached from below to continuum values when material cubic symmetry was considered. Comparison of the lowest normalized frequency between these to methods showed a better agreement for silicon nanostructures than that for germanium and carbon particles for which considerable differences were obtained. This different behavior is partially explained by noting that the parameters used in the molecular mechanics model have been calibrated for structure and energy calculations, and a better calibration may be required for vibrational analysis. The shape of the vibration modes obtained from molecular and continuum mechanics methods were practically the same for the sphere- and tetrahedron-shaped particles with the largest number of atoms. However, for cubes only the shape of the modes corresponding to

the lowest couple of frequencies were identical for both methods.

Finally, normalized natural frequencies obtained using the molecular dynamics approach increased as the solids were discretized into a larger number of mass points. Their magnitude approached to continuum values, and the number and groups of degenerate frequencies were exactly the same for these two methods. The latter behavior was expected because the potential energy constant for the molecular dynamics method were determined based on the components of the continuum elastic stiffness tensor. However, the excellent agreement with continuum values reported by the developers of this method was not achieved in this study [30]. It is believed that the simplifications made based on the assumption of small amplitude of vibrations, and the maximum number of mass points used in the discretization of the solids are the main causes of the poor agreement achieved between molecular dynamics and continuum mechanics methods.

Table 4.6 Normalized frequencies for silicon spheres obtained using molecular mechanics

Atoms	**123**	**227**	**477**	**933**	**Continuum**	
R (Å)	**7.3280**	**9.2000**	**12.8463**	**15.6620**	**Cubic**	**Isotropic**
1	1.5441	1.5465	1.9959	2.0415	2.1295	2.5011
2	1.5848	1.5465	1.9959	2.0415	2.1295	2.5011
3	1.5848	1.5465	1.9959	2.0415	2.1295	2.5011
4	1.5848	1.6093	2.3137	2.2895	2.1320	2.5011
5	1.7646	1.7145	2.3137	2.2895	2.1320	2.5011
6	1.7646	1.7145	2.3603	2.3910	2.4780	2.6361
7	2.0129	2.0738	2.3603	2.3910	2.4780	2.6361
8	2.0129	2.0738	2.5835	2.6449	2.6109	2.6361
9	2.0988	2.1062	2.7930	2.7467	2.6109	2.6361
10	2.0988	2.1062	2.7930	2.7467	2.6109	2.6361
11	2.0988	2.1062	2.7930	2.7467	2.9547	3.3639
12	2.4550	2.3844	2.9139	2.9716	2.9547	3.3639
13	2.4550	2.3844	2.9139	2.9716	2.9547	3.3639
14	2.4550	2.3844	2.9139	2.9716	3.1308	3.8647
15	2.5006	2.4258	3.1121	3.2225	3.4418	3.8647
16	2.5006	2.4258	3.1121	3.2225	3.4418	3.8647
17	2.5006	2.4258	3.1121	3.2225	3.4418	3.8647
18	2.8712	2.4858	3.2168	3.4871	3.5273	3.8647
19	2.8712	2.4858	3.2168	3.4871	3.5273	3.8647
20	2.9472	2.4858	3.2168	3.4871	3.5273	3.8647

Table 4.7 Normalized frequencies for germanium spheres obtained using molecular mechanics

Atoms	**123**	**227**	**477**	**933**	**Continuum**	
R (Å)	**7.6869**	**9.6155**	**13.4122**	**16.3476**	**Cubic**	**Isotropic**
1	1.8258	1.8623	2.3940	2.4458	2.0644	2.5011
2	1.9010	1.8623	2.3940	2.4458	2.0644	2.5011
3	1.9010	1.8623	2.3940	2.4458	2.0744	2.5011
4	1.9010	1.9043	2.7744	2.7396	2.0744	2.5011
5	2.1964	2.1292	2.7744	2.7396	2.0744	2.5011
6	2.1964	2.1292	2.8729	2.9138	2.4736	2.6341
7	2.4253	2.4846	2.8729	2.9138	2.4736	2.6341
8	2.4253	2.4846	3.0751	3.1465	2.6034	2.6341
9	2.6021	2.5968	3.3980	3.3412	2.6034	2.6341
10	2.6021	2.5968	3.3980	3.3412	2.6034	2.6341
11	2.6021	2.5968	3.3980	3.3412	2.8619	3.3336
12	2.9899	2.8792	3.5317	3.5935	2.8619	3.3336
13	2.9899	2.8792	3.5317	3.5935	2.8619	3.3336
14	2.9899	2.8792	3.5317	3.5935	3.0337	3.8647
15	3.0191	2.9641	3.7641	3.8953	3.3816	3.8647
16	3.0191	2.9641	3.7641	3.8953	3.3816	3.8647
17	3.0191	2.9641	3.7641	3.8953	3.3816	3.8647
18	3.4760	3.0231	3.9125	4.2337	3.4670	3.8647
19	3.4760	3.0231	3.9125	4.2337	3.4670	3.8647
20	3.5825	3.0231	3.9125	4.2337	3.4670	3.8647

Table 4.8 Normalized frequencies for carbon spheres obtained using molecular mechanics

Atoms	**123**	**227**	**477**	**933**	**Continuum**	
R (Å)	**4.8671**	**6.4076**	**8.5297**	**10.3863**	**Cubic**	**Isotropic**
1	1.6105	1.5840	2.0497	2.0707	2.3433	2.5011
2	1.6105	1.5840	2.0497	2.0707	2.3433	2.5011
3	1.6475	1.6565	2.0497	2.0977	2.3433	2.5011
4	1.6475	1.6565	2.0676	2.0977	2.3844	2.5011
5	1.6475	1.6565	2.0676	2.0977	2.3844	2.5011
6	1.7143	1.8585	2.3826	2.3292	2.4925	2.6129
7	1.8863	1.9496	2.3826	2.3292	2.4925	2.6129
8	1.8863	1.9496	2.3826	2.3292	2.5977	2.6129
9	1.8863	1.9496	2.5156	2.4846	2.5977	2.6129
10	2.1561	2.1603	2.5156	2.4846	2.5977	2.6129
11	2.1561	2.1603	2.5349	2.5585	2.8752	3.0451
12	2.1561	2.1603	2.5349	2.5585	2.8752	3.0451
13	2.1902	2.3541	2.5349	2.5585	2.8752	3.0451
14	2.1902	2.3541	2.8182	2.8770	3.1198	3.3381
15	2.3869	2.4643	2.8875	2.9069	3.5322	3.8285
16	2.5662	2.5248	2.9924	3.1446	3.6113	3.8285
17	2.5662	2.5248	2.9924	3.1446	3.6113	3.8285
18	2.5662	2.5248	2.9924	3.1446	3.6113	3.8285
19	2.8140	2.5299	3.0688	3.1621	3.6810	3.8285
20	2.8140	2.5299	3.0688	3.1621	3.6810	3.8285

Table 4.9 Normalized frequencies for silicon cubes obtained using molecular mechanics

Atoms	**64**	**216**	**512**	**1000**		
L (Å)	**9.5656**	**14.9988**	**20.4356**	**25.8838**	**Continuum**	
R (Å)	**5.9340**	**9.3045**	**12.6773**	**16.0570**	**Cubic**	**Isotropic**
1	0.9318	1.3749	1.6105	1.6875	1.7622	1.7723
2	1.1012	1.4325	1.6105	1.6875	1.7622	1.7723
3	1.1012	1.4325	1.6306	1.7547	1.9672	2.3724
4	1.2333	1.4884	1.6306	1.7547	1.9672	2.3724
5	1.2333	1.4884	1.6358	1.7948	1.9672	2.3724
6	1.2636	1.5123	1.6823	1.8087	2.2072	2.4224
7	1.4073	1.7407	1.9347	2.0819	2.2072	2.4224
8	1.4073	1.7407	1.9347	2.0819	2.2072	2.4224
9	1.5487	1.8465	2.0456	2.1785	2.3591	2.7081
10	1.6177	1.8465	2.1239	2.2632	2.3591	2.7081
11	1.6177	1.8478	2.1239	2.2632	2.3591	2.7081
12	1.6702	1.9330	2.1670	2.2702	2.3780	2.7561
13	1.6702	1.9608	2.1670	2.2736	2.3780	2.7561
14	1.7329	1.9608	2.1725	2.2736	2.3780	2.7561
15	1.7537	2.0112	2.2074	2.3922	2.5710	2.9082
16	1.8512	2.0112	2.2191	2.4179	2.5710	2.9082
17	1.8512	2.0318	2.2191	2.4179	2.5710	2.9082
18	1.9179	2.0440	2.3418	2.4465	2.6691	3.2045
19	1.9179	2.0440	2.3418	2.4465	2.6691	3.2045
20	2.0030	2.0519	2.3823	2.5590	2.9709	3.3975

Table 4.10 Normalized frequencies for germanium cubes obtained using molecular mechanics

Atoms	**64**	**216**	**512**	**1000**		
L (Å)	**9.9925**	**15.6652**	**21.3273**	**26.9892**	**Continuum**	
R (Å)	**6.1989**	**9.7179**	**13.2304**	**16.7427**	**Cubic**	**Isotropic**
1	1.0678	1.6117	1.9307	2.0745	1.7602	1.7722
2	1.3293	1.7241	1.9548	2.0745	1.7602	1.7722
3	1.3293	1.7241	1.9548	2.1022	1.9089	2.3698
4	1.4980	1.8032	1.9887	2.1022	1.9089	2.3698
5	1.5066	1.8388	1.9887	2.1369	1.9089	2.3698
6	1.5066	1.8388	2.0089	2.1470	2.1360	2.4217
7	1.7366	2.1240	2.3583	2.5307	2.1360	2.4217
8	1.7366	2.1240	2.3583	2.5307	2.1360	2.4217
9	1.9245	2.2396	2.4927	2.6441	2.3052	2.6852
10	1.9758	2.2396	2.5653	2.7228	2.3052	2.6852
11	1.9758	2.2673	2.5653	2.7228	2.3052	2.6852
12	2.0147	2.3363	2.6251	2.7472	2.3371	2.7561
13	2.0147	2.3646	2.6251	2.7472	2.3371	2.7561
14	2.0629	2.3646	2.6524	2.7616	2.3371	2.7561
15	2.1491	2.4377	2.6704	2.9011	2.5272	2.8963
16	2.2424	2.4377	2.6704	2.9102	2.5272	2.8963
17	2.2424	2.4647	2.6807	2.9102	2.5272	2.8963
18	2.3743	2.4770	2.8133	2.9424	2.5748	3.1767
19	2.3743	2.4770	2.8133	2.9424	2.5748	3.1767
20	2.4345	2.4935	2.8782	3.1155	2.9033	3.3924

Table 4.11 Normalized frequencies for carbon cubes obtained using molecular mechanics

Atoms	**64**	**216**	**512**	**1000**		
L (Å)	**6.3597**	**9.9605**	**13.5840**	**17.1774**	**Continuum**	
R (Å)	**3.9453**	**6.1790**	**8.4268**	**10.6560**	**Cubic**	**Isotropic**
1	1.0164	1.3224	1.4104	1.4612	1.7679	1.7718
2	1.0888	1.3224	1.4104	1.4612	1.7679	1.7718
3	1.0888	1.4886	1.6813	1.8053	2.1637	2.3420
4	1.2226	1.4886	1.6813	1.8053	2.1637	2.3420
5	1.2226	1.5035	1.7511	1.8649	2.1637	2.3420
6	1.3319	1.5870	1.8091	1.9550	2.3151	2.4128
7	1.3735	1.6679	1.8448	1.9767	2.3151	2.4128
8	1.3735	1.6856	1.8604	1.9767	2.3151	2.4128
9	1.3966	1.6856	1.8604	1.9957	2.3956	2.4732
10	1.5829	1.7892	1.9400	2.0210	2.3956	2.4732
11	1.5829	1.7893	1.9586	2.0316	2.3956	2.4732
12	1.6925	1.8244	1.9586	2.0316	2.5051	2.7561
13	1.7145	1.8605	2.0492	2.1775	2.5051	2.7561
14	1.7145	1.8605	2.0492	2.1775	2.5051	2.7561
15	1.7718	1.9217	2.1480	2.2285	2.6209	2.7819
16	1.7718	1.9493	2.1480	2.2285	2.6209	2.7819
17	1.8382	1.9493	2.1949	2.2743	2.6209	2.7819
18	1.8573	2.0268	2.2142	2.3676	2.6905	2.9300
19	1.8573	2.0268	2.2304	2.4353	2.6905	2.9300
20	1.8952	2.0760	2.2304	2.4353	2.8850	3.1076

Table 4.12 Normalized frequencies for silicon tetrahedrons obtained using molecular mechanics

Atoms	**51**	**136**	**281**	**502**	**815**		
a **(Å)**	**11.5125**	**19.1960**	**26.8761**	**34.5539**	**42.2301**	**Continuum**	
R (Å)	**3.5015**	**5.8384**	**8.1743**	**10.5094**	**12.8441**	**Cubic**	**Isotropic**
1	0.8821	1.0443	1.0940	1.1303	1.1588	1.2100	1.3038
2	0.8821	1.0443	1.0940	1.1303	1.1588	1.2100	1.3038
3	0.8821	1.0647	1.1677	1.2338	1.2800	1.3357	1.4484
4	0.9575	1.0647	1.1677	1.2338	1.2800	1.3357	1.4484
5	0.9575	1.0647	1.1677	1.2338	1.2800	1.3357	1.4484
6	1.1083	1.1887	1.2317	1.2644	1.2910	1.3602	1.5034
7	1.1147	1.1887	1.2317	1.2644	1.2910	1.3602	1.5034
8	1.1147	1.1887	1.2317	1.2644	1.2910	1.3602	1.5034
9	1.1147	1.4082	1.5863	1.7023	1.7832	1.9421	2.1677
10	1.3334	1.5761	1.7127	1.7989	1.8586	1.9731	2.2346
11	1.3334	1.5761	1.7127	1.7989	1.8586	1.9731	2.2346
12	1.4090	1.6841	1.8375	1.9088	1.9521	2.0373	2.2346
13	1.4090	1.6841	1.8375	1.9088	1.9521	2.0373	2.2824
14	1.4090	1.6841	1.8375	1.9088	1.9521	2.0373	2.2824
15	1.4152	1.7139	1.8425	1.9382	2.0096	2.1505	2.2824
16	1.4152	1.7139	1.8425	1.9382	2.0096	2.1505	2.3043
17	1.4152	1.7139	1.8425	1.9382	2.0096	2.1505	2.3043
18	1.7316	2.0229	2.1759	2.2802	2.3585	2.5153	2.6666
19	1.7316	2.0229	2.2072	2.3408	2.4381	2.8278	3.0259
20	1.7316	2.0229	2.2072	2.3408	2.4381	2.8278	3.0259

Table 4.13 Normalized frequencies for germanium tetrahedrons obtained using molecular mechanics

Atoms	**51**	**136**	**281**	**502**	**815**		
a **(Å)**	**12.0154**	**20.0380**	**28.0560**	**36.0709**	**44.0838**	**Continuum**	
R (Å)	**3.6544**	**6.0945**	**8.5331**	**10.9708**	**13.4079**	**Cubic**	**Isotropic**
1	1.0455	1.2638	1.3261	1.3712	1.4062	1.2033	1.2986
2	1.0455	1.2638	1.3261	1.3712	1.4062	1.2033	1.2986
3	1.0455	1.2732	1.4020	1.4844	1.5420	1.3231	1.4403
4	1.1530	1.2732	1.4020	1.4844	1.5420	1.3231	1.4403
5	1.1530	1.2732	1.4020	1.4844	1.5420	1.3231	1.4403
6	1.2926	1.4365	1.4913	1.5325	1.5656	1.3511	1.5026
7	1.3413	1.4365	1.4913	1.5325	1.5656	1.3511	1.5026
8	1.3413	1.4365	1.4913	1.5325	1.5656	1.3511	1.5026
9	1.3413	1.6672	1.8913	2.0373	2.1389	1.9278	2.1677
10	1.5961	1.8863	2.0520	2.1574	2.2306	1.9278	2.2261
11	1.5961	1.8863	2.0520	2.1574	2.2306	1.9280	2.2261
12	1.6394	2.0333	2.2084	2.2977	2.3548	2.0200	2.2261
13	1.6394	2.0333	2.2084	2.2977	2.3548	2.0200	2.2769
14	1.6394	2.0333	2.2084	2.2977	2.3548	2.0200	2.2769
15	1.7007	2.0359	2.2253	2.3489	2.4364	2.1496	2.2769
16	1.7007	2.0359	2.2253	2.3489	2.4364	2.1496	2.2990
17	1.7007	2.0359	2.2253	2.3489	2.4364	2.1496	2.2990
18	2.0517	2.3959	2.6279	2.7780	2.8735	2.4865	2.6407
19	2.0517	2.3959	2.6279	2.7971	2.9205	2.8202	3.0118
20	2.0517	2.3959	2.6279	2.7971	2.9205	2.8202	3.0118

Table 4.14 Normalized frequencies for carbon tetrahedrons obtained using molecular mechanics

Atoms	**51**	**136**	**281**	**502**	**815**		
a **(Å)**	**7.5635**	**12.6377**	**17.7171**	**22.7996**	**27.8841**	**Continuum**	
R (Å)	**2.3004**	**3.8437**	**5.3886**	**6.9344**	**8.4808**	**Cubic**	**Isotropic**
1	0.8936	0.9546	0.9821	1.0049	1.0240	1.2080	1.2488
2	0.8936	0.9546	0.9821	1.0049	1.0240	1.2080	1.2488
3	0.8936	1.0512	1.0917	1.1118	1.1290	1.3112	1.3637
4	0.9165	1.0512	1.0917	1.1118	1.1290	1.3112	1.3637
5	0.9165	1.0512	1.0917	1.1118	1.1290	1.3112	1.3637
6	1.0281	1.0673	1.1346	1.1862	1.2217	1.4412	1.4942
7	1.0281	1.0673	1.1346	1.1862	1.2217	1.4412	1.4942
8	1.0281	1.0673	1.1346	1.1862	1.2217	1.4412	1.4942
9	1.1834	1.4503	1.5993	1.6936	1.7584	2.0580	2.1465
10	1.3029	1.5055	1.6240	1.7031	1.7599	2.0580	2.1465
11	1.3029	1.5055	1.6240	1.7031	1.7599	2.0580	2.1465
12	1.3029	1.5055	1.6240	1.7031	1.7599	2.0791	2.1677
13	1.3615	1.6057	1.7275	1.7918	1.8124	2.1176	2.2204
14	1.3615	1.6081	1.7349	1.7918	1.8124	2.1176	2.2204
15	1.4047	1.6081	1.7349	1.7918	1.8124	2.1668	2.2204
16	1.4907	1.7084	1.7640	1.8080	1.8550	2.1668	2.2540
17	1.4907	1.7084	1.7640	1.8080	1.8550	2.1668	2.2540
18	1.4907	1.7084	1.7640	1.8116	1.8735	2.2938	2.3948
19	1.7025	2.0076	2.1594	2.2453	2.2986	2.8106	2.8919
20	1.7025	2.0076	2.1594	2.2453	2.2986	2.8106	2.8919

Table 4.15 Normalized frequencies for silicon spheres with assumed material isotropic symmetry obtained from molecular dynamics

Points	**312**	**624**	**1064**	**1640**	**2368**	**7736**	**Continuum**
R (Å)	**10.00**	**10.00**	**10.00**	**10.00**	**10.00**	**10.00**	**Isotropic**
1	1.7161	1.8948	1.9516	2.0313	2.0926	2.2326	2.5011
2	1.7161	1.8948	1.9516	2.0313	2.0926	2.2326	2.5011
3	1.8376	1.9248	2.0208	2.0827	2.1504	2.2602	2.5011
4	1.8376	1.9248	2.0208	2.0827	2.1504	2.2602	2.5011
5	1.8376	1.9248	2.0208	2.0827	2.1504	2.2602	2.5011
6	2.0925	2.1753	2.2359	2.2984	2.3529	2.4488	2.6361
7	2.0925	2.1753	2.2359	2.2984	2.3529	2.4488	2.6361
8	2.0925	2.1753	2.2359	2.2984	2.3529	2.4488	2.6361
9	2.1369	2.1930	2.2599	2.3161	2.3699	2.4561	2.6361
10	2.1369	2.1930	2.2599	2.3161	2.3699	2.4561	2.6361
11	2.4572	2.6659	2.7449	2.8448	2.9224	3.0720	3.3639
12	2.4572	2.6659	2.7449	2.8448	2.9224	3.0720	3.3639
13	2.4572	2.6659	2.7449	2.8448	2.9224	3.0720	3.3639
14	2.4620	2.6926	2.9381	3.0307	3.1713	3.4011	3.8647
15	2.4620	2.7997	2.9381	3.0965	3.2317	3.4350	3.8647
16	2.4620	2.7997	2.9381	3.0965	3.2317	3.4350	3.8647
17	2.5381	2.7997	3.0238	3.0965	3.2317	3.4350	3.8647
18	2.5607	3.0053	3.0251	3.1811	3.2496	3.4684	3.8647
19	2.5607	3.0053	3.0251	3.1811	3.2496	3.4684	3.8647
20	2.5607	3.0053	3.0251	3.1811	3.2496	3.4684	3.8647

Table 4.16 Normalized frequencies for silicon spheres with assumed material cubic symmetry obtained from molecular dynamics

Points	**312**	**624**	**1064**	**1640**	**2368**	**7736**	**Continuum**
R (Å)	**10.00**	**10.00**	**10.00**	**10.00**	**10.00**	**10.00**	**Cubic**
1	1.4886	1.5937	1.6732	1.7332	1.7920	1.9006	2.1295
2	1.4886	1.5937	1.6732	1.7332	1.7920	1.9006	2.1295
3	1.4886	1.5937	1.6732	1.7332	1.7920	1.9006	2.1295
4	1.7010	1.7561	1.8152	1.8602	1.9055	1.9790	2.1320
5	1.7010	1.7561	1.8152	1.8602	1.9055	1.9790	2.1320
6	1.7070	1.8767	1.9413	2.0197	2.0834	2.2181	2.4780
7	1.7070	1.8767	1.9413	2.0197	2.0834	2.2181	2.4780
8	2.0372	2.0219	2.2090	2.2774	2.3294	2.4248	2.6109
9	2.0372	2.1563	2.2090	2.2774	2.3294	2.4248	2.6109
10	2.0372	2.1563	2.2090	2.2774	2.3294	2.4248	2.6109
11	2.0646	2.1563	2.2939	2.3309	2.4590	2.6816	2.9547
12	2.1059	2.3384	2.3875	2.4944	2.5597	2.6955	2.9547
13	2.1059	2.3384	2.3875	2.4944	2.5597	2.6955	2.9547
14	2.1059	2.3384	2.3875	2.4944	2.5597	2.6955	3.1308
15	2.1323	2.5780	2.6048	2.7578	2.8245	3.0514	3.4418
16	2.1323	2.5780	2.6048	2.7578	2.8245	3.0514	3.4418
17	2.1323	2.5780	2.6048	2.7578	2.8245	3.0514	3.4418
18	2.2929	2.7015	2.8369	2.9904	3.1183	3.2626	3.5273
19	2.2929	2.7015	2.8369	2.9904	3.1183	3.2626	3.5273
20	2.3281	2.7015	2.8369	2.9904	3.1183	3.2626	3.5273

Table 4.17 Normalized frequencies for silicon cubes with assumed material isotropic symmetry obtained from molecular dynamics

Points	**343**	**729**	**1331**	**2197**	**8000**	
L (Å)	**16.120**	**16.120**	**16.120**	**16.120**	**16.120**	**Continuum**
R (Å)	**10.00**	**10.00**	**10.00**	**10.00**	**10.00**	**Isotropic**
1	1.4657	1.5395	1.5851	1.6159	1.6732	1.7723
2	1.4657	1.5395	1.5851	1.6159	1.6732	1.7723
3	1.8159	1.9306	2.0064	2.0602	2.1664	2.3724
4	1.8159	1.9306	2.0064	2.0602	2.1664	2.3724
5	1.8159	1.9306	2.0064	2.0602	2.1664	2.3724
6	1.9673	2.0998	2.1621	2.2044	2.2837	2.4224
7	1.9994	2.0998	2.1621	2.2044	2.2837	2.4224
8	1.9994	2.0998	2.1621	2.2044	2.2837	2.4224
9	1.9994	2.1210	2.2250	2.3000	2.4513	2.7081
10	2.1776	2.2966	2.3720	2.4241	2.5243	2.7081
11	2.1776	2.2966	2.3720	2.4241	2.5243	2.7081
12	2.1776	2.2966	2.3720	2.4241	2.5243	2.7561
13	2.2392	2.3742	2.4464	2.4958	2.5892	2.7561
14	2.2392	2.3742	2.4464	2.4958	2.5892	2.7561
15	2.2392	2.3846	2.4787	2.5443	2.6717	2.9082
16	2.2586	2.3846	2.4787	2.5443	2.6717	2.9082
17	2.2586	2.3846	2.4787	2.5443	2.6717	2.9082
18	2.4595	2.6179	2.7211	2.7935	2.9355	3.2045
19	2.4595	2.6179	2.7211	2.7935	2.9355	3.2045
20	2.4881	2.6949	2.8303	2.9255	3.1110	3.3975

Table 4.18 Normalized frequencies for silicon cubes with assumed material cubic symmetry obtained from molecular dynamics

Points	**343**	**729**	**1331**	**2197**	**8000**	
L (Å)	**16.120**	**16.120**	**16.120**	**16.120**	**16.120**	**Continuum**
R (Å)	**10.00**	**10.00**	**10.00**	**10.00**	**10.00**	**Cubic**
1	1.3768	1.5107	1.5694	1.6012	1.6602	1.7622
2	1.3938	1.5107	1.5694	1.6012	1.6602	1.7622
3	1.3938	1.5107	1.5884	1.6437	1.7518	1.9672
4	1.3938	1.5224	1.5884	1.6437	1.7518	1.9672
5	1.4461	1.5224	1.5884	1.6437	1.7518	1.9672
6	1.4461	1.5365	1.6454	1.7242	1.8817	2.2072
7	1.7523	1.8694	1.9339	1.9778	2.0583	2.2072
8	1.7523	1.8694	1.9339	1.9778	2.0583	2.2072
9	1.7523	1.8971	1.9888	2.0512	2.1664	2.3591
10	1.7647	1.8971	1.9888	2.0512	2.1664	2.3591
11	1.7647	1.8971	1.9888	2.0512	2.1664	2.3591
12	1.8676	1.9836	2.0565	2.1067	2.2014	2.3780
13	1.8676	1.9836	2.0565	2.1067	2.2014	2.3780
14	1.8676	1.9836	2.0565	2.1067	2.2014	2.3780
15	1.9417	2.1050	2.2042	2.2741	2.3764	2.5710
16	1.9417	2.1050	2.2042	2.2741	2.3764	2.5710
17	1.9417	2.1561	2.2310	2.2800	2.3764	2.5710
18	1.9539	2.1561	2.2310	2.2800	2.4092	2.6691
19	1.9539	2.1561	2.2310	2.2800	2.4092	2.6691
20	2.0528	2.1613	2.2988	2.4000	2.5967	2.9709

Table 4.19 Normalized frequencies for pentahedral silicon pyramids with assumed material isotropic symmetry obtained from molecular dynamics

Points	**406**	**904**	**1690**	**6416**	
H (Å)	**14.646**	**14.646**	**14.646**	**14.646**	**Continuum**
R (Å)	**10.00**	**10.00**	**10.00**	**10.00**	**Isotropic**
1	0.5437	0.5681	0.5861	0.6212	0.7251
2	0.6849	0.7358	0.7732	0.8443	1.0403
3	0.7743	0.8095	0.8359	0.8880	1.0558
4	0.8702	0.9096	0.9389	0.9970	1.1900
5	0.8702	0.9096	0.9389	0.9970	1.1900
6	1.1026	1.1879	1.2442	1.3407	1.5716
7	1.1026	1.1879	1.2442	1.3407	1.5716
8	1.2026	1.2680	1.3131	1.4011	1.7135
9	1.2026	1.2680	1.3131	1.4011	1.7135
10	1.2551	1.3053	1.3467	1.4366	1.7495
11	1.3010	1.3614	1.3999	1.4771	1.7509
12	1.3094	1.3738	1.4182	1.4935	1.7721
13	1.3135	1.4082	1.4723	1.5855	1.8850
14	1.4421	1.5303	1.5801	1.6765	1.9350
15	1.4648	1.5647	1.6476	1.7912	2.1156
16	1.5421	1.6698	1.7494	1.8830	2.2951
17	1.5421	1.6698	1.7494	1.8830	2.2951
18	1.6181	1.7774	1.8721	1.9965	2.3795
19	1.7027	1.8222	1.8846	2.0216	2.4442
20	1.7562	1.8315	1.9022	2.0321	2.5006

Table 4.20 Normalized frequencies for pentahedral silicon pyramids with assumed material cubic symmetry obtained from molecular dynamics

Points	**406**	**904**	**1690**	**6416**	
H (Å)	**14.646**	**14.646**	**14.646**	**14.646**	**Continuum**
R (Å)	**10.00**	**10.00**	**10.00**	**10.00**	**Cubic**
1	0.4987	0.5553	0.5778	0.6129	0.7170
2	0.5354	0.5598	0.5955	0.6695	0.8628
3	0.6873	0.7224	0.7481	0.7979	0.9526
4	0.7744	0.8201	0.8532	0.9168	1.1143
5	0.7744	0.8201	0.8532	0.9168	1.1143
6	0.8757	0.9547	1.0086	1.1037	1.3406
7	0.8757	0.9547	1.0086	1.1037	1.3406
8	0.9543	1.0474	1.1123	1.2070	1.5193
9	0.9923	1.0619	1.1125	1.2070	1.5193
10	0.9953	1.0639	1.1125	1.2186	1.5428
11	0.9953	1.0639	1.1139	1.2299	1.5711
12	1.1329	1.2437	1.2995	1.3711	1.6266
13	1.2140	1.2637	1.3187	1.4068	1.6703
14	1.2341	1.2953	1.3347	1.4485	1.7394
15	1.3465	1.4461	1.5176	1.6339	1.8879
16	1.3477	1.4643	1.5256	1.6579	2.0991
17	1.3477	1.4886	1.5753	1.7126	2.1345
18	1.3590	1.4947	1.5772	1.7126	2.1480
19	1.3757	1.4947	1.5772	1.7269	2.1480
20	1.4333	1.5406	1.6158	1.7521	2.1887

Chapter 5
Summary and Conclusions

The main objectives of this work were to 1) evaluate the size dependence of the vibrational properties of particles at the nanoscale, and 2) evaluate the applicability of the continuum mechanics assumption to determine their natural frequencies and mode shapes. To achieve this goal, the vibrational spectra of nanostructures with different shapes, sizes, and made of different materials has been studied using three different methods: molecular mechanics, molecular dynamics, and continuum mechanics.

Molecular mechanics is an atomistic approach to model molecular structures. In these method, the atoms are connected by bonds that describe all possible interactions. These interactions are expressed in terms of potential energy functions, which are stated as functions of different parameters. These parameters are determined by calibration to reproduce experimental data or to match results obtained using the more sophisticated quantum mechanics method. This method begins with the optimization of the structure to find the equilibrium geometry, which corresponds to the lowest possible energy level. Then, the natural frequencies of vibration and the respective modes are determined by assuming harmonic motion, and solving the resulting eigenvalue problem.

The molecular dynamics approach employed in this study is based on the work presented by Saviot et al. [22]. In their approach, the solid of arbitrary shape is constructed from a crystal cubic lattice of mass points connected by springs. Saviot and co-workers proposed harmonic functions to state the potential energy equations

describing the coupling between first, second, third, and so on neighbors, as well as the octet interactions. They showed that only three interaction terms are needed to reproduce the behavior of a general cubically elastic material, and reported the constants for the potential energy equations in terms of the parameters C_{11}, C_{12}, and C_{44} of the continuum material. Based on this potential energy equations, combined with the Euler-Lagrange equations, and assuming harmonic motion the general eigenvalue problem was obtained, and then solved to evaluated the natural vibrational frequencies and modes of the nanoparticles.

The equations of motion for a general anisotropic linearly elastic material form the base for the continuum mechanics method. The weak form of the governing equations is determined using a variational approach. The resulting differential equations are not directly solved, instead, using the Ritz method, approximate solutions are obtained, and expressions for the displacements are approximated as finite linear combinations of power series. The final eigenvalue problem is obtained by assuming harmonic motion.

Molecular mechanics was used to determine the natural frequencies of sphere-, cube-, and tetrahedron-shaped nanoparticles. Pyramid-shaped nanostructures were not analyzed using this approach because that is not a shape that the materials considered in this study would naturally form at the nanoscale level due to its crystal geometric structure. On the other hand, the natural frequencies of sphere-, cube-, and pyramid-shaped silicon nanoparticles having isotropic and cubic symmetries were calculated using molecular dynamics, and tetrahedron-shaped nanostructures were not considered because the molecular dynamics approach employed here is based on

a cubic lattice with which is not possible to reproduce all the geometric symmetries of a tetrahedron.

Three different materials were considered in this study: silicon, germanium, and carbon, with the purpose of reviewing the influence of the element properties on the nanostructure vibrational properties as we move from one row to the next one in the periodic table within the same group.

The primary features and most important conclusions obtained from this work related with the vibrational behavior of the nanostructures with shapes, made of the materials, and using the analytical methods considered in this work are as follows

1. There is a dependence of the behavior of particles on the size at the nanoscale. In particular, the magnitude of the frequencies, and the number and groups of degenerate frequencies change with the size of the particle.

2. Normalized frequencies increase non-linearly with the number of atoms forming the particle. The latter indicates, as a consequence, that the equivalent continuum elastic stiffness constants also depend on the size for particles at this scale.

3. Normalized frequencies increase linearly as a function of the size of the nanoparticles. The latter indicates that the scale invariance of the normalized frequency in continuum elasticity does not hold for the range of particles sizes considered in this study.

4. The variation with size of the lowest normalized frequency for spherical nanoparticles was not smooth when the molecular mechanics method was employed.

This is explained by the fact that due to the crystal structure of the materials considered, the geometry of the molecular models is not perfectly spherical, and it actually changes as the number of atoms is increased.

5. The lowest frequency for cube- and tetrahedron-shaped structures obtained using molecular mechanics exhibited a smooth variation with the number of atoms forming the particle, allowing the fitting of a second order polynomial. The variation of the lowest normalized frequencies with the size of the particle is also smooth, and linear equations describing this behavior were obtained from least-square curve fitting.

6. The converged values for the lowest normalized frequency of cube-shaped nanoparticles according to the fitted second order polynomials are 1.793, 2.22, and 1.50 for silicon, germanium, and carbon, respectively. Compared with the lowest continuum mechanics frequency obtained assuming cubic symmetry, these values are only 1.8% lower for silicon, 26% higher for germanium, and 15% lower for carbon cubes.

7. The converged values for the lowest normalized frequency of tetrahedron-shaped nanoparticles according to the fitted second order polynomials are 1.175, 1.46, and 1.04 for silicon, germanium, and carbon, respectively. Compared with the lowest continuum mechanics frequency obtained assuming cubic symmetry, these values are only 2.9% lower for silicon, 21.3% higher for germanium, and 13.9% lower for carbon cubes.

8. There is a better fitting for silicon than there is for germanium and carbon

nanoparticles. This behavior may be explained by the fact that the parameters used in the interatomic potential of the molecular mechanics method were not mainly determined for vibrational analyses, and a better calibration is required. This task can be accomplished by fitting the available vibrational spectroscopy data, and if needed, by introducing additional parameters in the interatomic potential functions.

9. Normalized frequencies of nanoparticles may be estimated using the proposed equations for the shapes, size range, and materials considered here.

10. Vibrational mode shapes match between molecular and continuum mechanics methods for the particles composed by the higher considered number of atoms, at least for the lowest of frequencies. This is an indication that the frequencies should also match if frequencies for particles formed by a sufficient number of atoms are determined.

11. The validity of the continuum mechanics assumption for determining the vibrational spectra of particles at the nanoscale depends not only on the size, but also on the material of which the nanostructure is made.

12. Initial estimates of the lowest vibrational frequencies of nanostructures may be obtained using continuum mechanics. However, a more accurate method such as quantum mechanics must be used for final analyses or rigorous conclusions.

13. The normalized natural frequencies for silicon particles obtained using the molecular dynamics approach proposed by Saviot et. al [22] increase as the solid is discretized into a larger number of mass points.

14. According to the present work, molecular dynamics normalized frequencies approach to continuum values from below. However, for the maximum number of points considered here, agreement between these methods was not achieved. It is believed that the simplifications made based on the assumption of small amplitude of vibrations, and the maximum number of mass points used in the discretization of the solids are the main causes of the poor agreement achieved between molecular dynamics and continuum mechanics methods. Therefore, the molecular dynamics approach is expected to be able to recover the continuum frequencies, as reported in the literature [30], when the solids are discretized using a sufficient number of mass points.

15. The number and groups of degenerate frequencies were identical between molecular dynamics and continuum mechanics methods for all the geometries studied. This behavior was expected since the parameters of this method were determined to replicate the components of the linear elastic stiffness tensor.

References

1. Rufo, S., Dutta, M., and Stroscio, M.A. (2003) Acoustic modes in free and embedded quantum dots. *Journal of Applied Physics*,**93**(5):2900-2905.

2. Fujii, M. Nagareda, T., Hayashi S., and Yamamoto K. (1991) Low-frequency Raman scattering from small silver particles embedded in SiO_2 thin films. *Physical Review B*, **44**(12):6243-6248.

3. Tamura, A., Higeta, K., and Ichinokawa, T. (1982) Lattice vibrations and specific heat of a small particle. *Journal of Physics C:Solid State*, **15**:4975-4991.

4. Lamb, H. (1882). On the vibrations of an elastic sphere. *Proceedings of the London Mathematical Society* **13**:189-212.

5. Tanaka, A., Onari, S., and Arai, T. (1993) Low-freqeuncy Raman scattering from CdS microcrystals embedded in a germanium dioxide glass matrix. *Physical Review B*, **47**(3):1237-1243.

6. Ovisuk, N.N., and Novikov, V.N. (1996) Influence of a glass matrix on acoustic phonons confined in microcrystals. *Physical review B*, **53**(6):3113-3118.

7. Verma, P., Cordts, W., Irmer, G., and Monecke, J. (1999) Acoustic vibrations of semiconductor nanocrystals in doped glasses. *Physical review B*, **60**(8):5778-5785.

8. Saviot, L., Champagnon, B., Duval, E.,Kudriavtsev,I.A., and Ekimov, A.I. (1996) Size dependence of acoustic and optical vibrational modes of CdSe nanocrystals in glasses. *Journal of Non-Crystalline Solids*, **197**:238-246.

9. Saviot, L., Murray, D.B., and Marco de Lucas, M.C. (2004) Vibrations of free and embedded elastic spheres: Application to low-frequency Raman scattering of silicon nanoparticles in silica. *Physical Review B*, **69**:113402.

10. A. K. Rappe', C. J. Casewit, K. S. Colwell, W. A. Goddard III, and W. M. Skiff. (1992)UFF, a Rule-Based Full Periodic Table Force Field for Molecular Mechanics and Molecular Dynamics Simulations. *J. Am. Chem. Soc*, **114**:10024.

11. C. J. Casewit, K. S. Colwell, and A. K. Rappe'. (1992) Application of a Universal Force Field to Organic Molecules. *J. Am. Chem. Soc*, **114**:10035.

12. C. J. Casewit, K. S. Colwell, and A. K. Rappe'. (1992) Application of a Universal Force Field to Organic Molecules. *J. Am. Chem. Soc*, **114**:10046.

13. K. Rappe', K. S. Colwell, and C. J. Casewit. (1993) Application of a Universal Force Field to Metallic Complexes. A. *Inorg. Chem.*, **32**:3438.

14. Murrell, J. N., Sorbie, K. S. (1974) New analytic form for the potential energy curves of stable diatomic states *J. Chem. Soc., Faraday Trans.* **2**(70):1552-1557.

15. Huxley, P.; Murrell, J. N. (1983) Ground-state diatomic potentials. *J. Chem. Soc., Faraday Trans.*, **2**(79):323-328.

16. Ermakov, K. V., Butayev, B.S., and Spiridonov, V.P. (1990) Model potential functions of nonlinear XY_2 2 molecules *J. Mol. Struct.*,**240**:295-303.

17. Stillinger, F.H., and Weber, T.A. (1985) Computer simulation of local order in condensed phases of silicon. *Physical Review B*, **31**:5262-5271.

18. Pack R.T., Valentini, J.J., Becker, C.H., Buss, R.J., and Lee, Y.T. (1982) Multiproperty empirical interatomic potentials for ArXe and KrXe^a. *Journal of Chemical Physics*,**77**(11):5475-5485.

19. Pack R.T., Valentini, J.J., and Cross, J.B. (1982) Multiproperty empirical anisotropic intermolecular potentials for $ArSF_6$ and $KrSF_6^a$ *Journal of Chemical Physics*,**77**(11):5486-5499.

20. Rappe, A.K., and Casewit, C.J. Molecular Mechanics Across Chemistry. University Science Books, Sausalito, CA, 1997.

21. Wilson, E.B., Decious, J.C., Cross, P.C., Molecular Vibrations. Dover Publications Inc., New York, 1980.

22. Murray, D. B. and Saviot, L. (2004). Phonons in an inhomogeneous medium: Vibrations of an embedded nanoparticle. *Physical Review B* **69**:094305.

23. Reddy, J.N. (1984). *Energy and Variational Methods in Applied Mechanics*. Wiley, New York.

24. Visscher, W.M., Migliori, A., Bell, T.M., and Reinert, R.A. (1991) On the normal modes of free vibration in inhomogeneous nad anisotropic elastic objects. *J. Acoust. Soc. Am* **90**:2154.

25. Heyliger, P.R., Pan, E., Cook, S., and Manaloto, M. (2004) Acoustic modes of anisotropic nanoparticles: spheres, cubes and pyramids. *Journal of Nanoscience and nanotechnology*, In press.

26. Heyliger, P. R. and Kienholz, J. (2005). The Mechanics of Pyramids. *International Journal of Solids and Structures* Available online 12 September 2005.

27. Allinger, Nl. Yuh, Yh., Lii, Jh. (1989) Molecular Mechanics - The Mm3 Force-Field For Hydrocarbons 1. *Journal Of The American Chemical Society*, **111**:8551.

28. Lii, Jh., and Allinger, Nl. (1989) Molecular Mechanics - The Mm3 Force-Field For Hydrocarbons .2. Vibrational Frequencies And Thermodynamics. *Journal Of The American Chemical Society* **111**:8566.

29. New Semiconductor Materials. Characteristics and Properties. Loffe Physico-Technical Institute. http://www.ioffe.rssi.ru/SVA/NSM/

30. Murray, M. (2003) Eight point force molecular dynamical estimates of vibrational frequencies of an isotropic elastic sphere.

http://www.geocities.com/cofrest/md12.htm